NAVAL POSTGRADUATE SCHOOL

MONTEREY, CALIFORNIA

THESIS

MEASUREMENT OF MINORITY CHARGE CARRIER DIFFUSION LENGTH IN GALLIUM NITRIDE NANOWIRES USING ELECTRON BEAM INDUCED CURRENT (EBIC)

by

Chiou Perng Ong

December 2009

Thesis Advisor: Nancy M. Haegel
Second Reader: Gamani Karunasiri

Approved for public release; distribution is unlimited

REPORT DOCUMENTATION PAGE		Form Approved OMB No. 0704-0188

1. AGENCY USE ONLY *(Leave blank)*	2. REPORT DATE December 2009	3. REPORT TYPE AND DATES COVERED Master's Thesis

4. TITLE AND SUBTITLE Measurement of Minority Charge Carrier Diffusion Length in Gallium Nitride Nanowires Using Electron Beam Induced Current (EBIC)	5. FUNDING NUMBERS DMR 0804527
6. AUTHOR(S) Ong, Chiou Perng	
7. PERFORMING ORGANIZATION NAME(S) AND ADDRESS(ES) Naval Postgraduate School Monterey, CA 93943-5000	8. PERFORMING ORGANIZATION REPORT NUMBER
9. SPONSORING /MONITORING AGENCY NAME(S) AND ADDRESS(ES) N/A	10. SPONSORING/MONITORING AGENCY REPORT NUMBER

11. SUPPLEMENTARY NOTES The views expressed in this thesis are those of the author and do not reflect the official policy or position of the Department of Defense or the U.S. government.

12a. DISTRIBUTION / AVAILABILITY STATEMENT Approved for public release; distribution is unlimited	12b. DISTRIBUTION CODE A

13. ABSTRACT (maximum 200 words)

Electron Beam Induced Current (EBIC) measurements were performed on GaN nanowires to determine minority charge carrier diffusion length, L_d. Although EBIC has been used to characterize bulk and thin film materials, very little is known about near contact transport in GaN nanowires. The results obtained from EBIC will be compared against those obtained from a novel Near-field Scanning Optical Microscopy (NSOM) method developed at the Naval Postgraduate School (NPS) that provides an alternative method for the determination of L_d. Two types of nanowires were investigated: n-type GaN/AlGaN (core-shell) nanowires and unintentionally doped (UID) n-type GaN uncoated nanowires. By exciting the nanowires using an electron beam in the SEM, the EBIC signal collected at the metal-semionductor Schottky contact represents a diffusive current. Diffusion length can then be extracted from the spatial variation of the EBIC signal. The diffusion length of holes in the GaN/AlGaN wires was measured to be 1.2 μm ± 22% and the diffusion length of holes in the UID GaN uncoated wires was measured to be 0.40 μm ± 24%. The results demonstrate the dependence of diffusion length on the diameter and surface behavior of the nanowire.

14. SUBJECT TERMS Minority charge carrier, diffusion length, GaN, nanowires, EBIC.	15. NUMBER OF PAGES 93
	16. PRICE CODE

17. SECURITY CLASSIFICATION OF REPORT	18. SECURITY CLASSIFICATION OF THIS PAGE	19. SECURITY CLASSIFICATION OF ABSTRACT	20. LIMITATION OF ABSTRACT
Unclassified	Unclassified	Unclassified	UU

NSN 7540-01-280-5500 Standard Form 298 (Rev. 8-98)
Prescribed by ANSI Std. Z39.18

THIS PAGE INTENTIONALLY LEFT BLANK

Approved for public release; distribution is unlimited

MEASUREMENT OF MINORITY CHARGE CARRIER DIFFUSION LENGTH IN GALLIUM NITRIDE NANOWIRES USING ELECTRON BEAM INDUCED CURRENT (EBIC)

Chiou Perng Ong
Major, Singapore Armed Forces
B. App. Sc in Electrical Eng (Class 2), University of British Columbia, 2004

Submitted in partial fulfillment of the
requirements for the degree of

MASTER OF SCIENCE IN COMBAT SYSTEMS SCIENCE AND TECHNOLOGY

from the

NAVAL POSTGRADUATE SCHOOL
December 2009

Author: Chiou Perng Ong

Approved by: Nancy M. Haegel
Thesis Advisor

Gamani Karunasiri
Second Reader

Andres Larraza, PhD
Chairman, Department of Physics

THIS PAGE INTENTIONALLY LEFT BLANK

ABSTRACT

Electron Beam Induced Current (EBIC) measurements were performed on GaN nanowires to determine minority charge carrier diffusion length, L_d. Although EBIC has been used to characterize bulk and thin film materials, very little is known about near contact transport in GaN nanowires. The results obtained from EBIC will be compared against those obtained from a novel Near-field Scanning Optical Microscopy (NSOM) method developed at the Naval Postgraduate School (NPS) that provides an alternative method for the determination of L_d. Two types of nanowires were investigated: n-type GaN/AlGaN (core-shell) nanowires and unintentionally doped (UID) n-type GaN uncoated nanowires. By exciting the nanowires using an electron beam in the SEM, the EBIC signal collected at the metal-semionductor Schottky contact represents a diffusive current. Diffusion length can then be extracted from the spatial variation of the EBIC signal. The diffusion length of holes in the GaN/AlGaN wires was measured to be 1.2 μm ± 22% and the diffusion length of holes in the UID GaN uncoated wires was measured to be 0.40 μm ± 24%. The results demonstrate the dependence of diffusion length on the diameter and surface behavior of the nanowire.

THIS PAGE INTENTIONALLY LEFT BLANK

TABLE OF CONTENTS

LIST OF FIGURES

LIST OF TABLES

THIS PAGE INTENTIONALLY LEFT BLANK

ACKNOWLEDGMENTS

I would like to show my most sincere appreciation to my thesis advisor, Professor Nancy Haegel, for her invaluable guidance, unmatched patience, and endless encouragement. It is her belief that “All data is good data”, that has made many of the observations possible. The thesis would not have accomplished so much if not for her leadership and persistence. Coupled with her approachable personality, the learning experience in these twelve months has been enriching and fruitful. I would also like to thank my co-advisor, Professor Karunasiri, for his efforts in ensuring the high quality of this thesis.

I am also grateful to the help I have received from LCDR Lee Baird and LCDR Mike Touse. Lee has made my work much easier by being the knowledge repository of all sample related matters and being so skilled at operating all the equipment available in the laboratory. Mike has spent many hours, unconditionally, on the wire-bonding machine, trying to make the nanowire samples experiment worthy.

My appreciation extends to Dr George Wang for the GaN nanowires, without which this thesis work would not be possible. I would also like to thank Mr Sam Bourne and Mr George Jaksha for their contributions in making the thesis work possible. This work is supported by the National Science Foundation through Grant DMR-0804527.

To my wife, Kristene, thank you for the support and understanding; for the long hours, late nights, and burnt weekends. Without you, this journey would not have been this smooth.

THIS PAGE INTENTIONALLY LEFT BLANK

I. INTRODUCTION

A. BACKGROUND

The term “Nanotechnology” was first defined in 1974 by Professor Norio Taniguchi from Tokyo Science University as the process of separating, consolidating and deforming materials by one atom or by one molecule [1]. However, the idea of having the ability to precisely manipulate individual atoms and molecules had already made its first “public appearance” during the talk “There’s Plenty of Room at the Bottom” given by physicist Dr Richard Feynman at an American Physical Society meeting at the California Institute of Technology in 1959 [2]. The development of nanotechnology has come a long way since Professor Tanuguchi provided this definition. Today, nanotechnology can be applied in almost any fields ranging from drug delivery in medicine, to memory storage in information and communication, to nonwoven textiles in the textile industry and to enhanced armor protection in military applications.

One of the basic building blocks of many nanodevices is the nanowire. While there is extensive work aimed at improving the growth of nanowires, the characterization of these devices is equally important. The optical, electrical and even chemical properties of these nanowires will be the underlying foundation in their applications in opto- and nano-electronics, photovoltaic devices and chemical and biological sensors. This thesis emphasizes characterization of the diffusion length of minority charge carriers in Gallium Nitride (GaN) nanowires, using a technique called Electron Beam Induced Current (EBIC).

GaN is a Group III/Group V compound which has a large (3.4 eV) direct bandgap. This big bandgap makes it a good material choice for optoelectronic, high powered, high frequency devices. Coupled with its low sensitivity to ionizing radiation, GaN is also suitable for making solar cells. GaN is also used in the

manufacturing of lasers. An example is the GaN laser diode used in Blu-ray disc technology. GaN's large bandgap creates emission in the blue-UV part of the spectrum.

B. THE PURPOSE OF THIS THESIS

This thesis has two main objectives. First, this thesis aims to measure the diffusion length of minority charge carriers in GaN nanowires. While there are many reports on minority charge carrier diffusion in GaN bulk materials, dating as early as the 1950s, little can be found in the literature regarding the diffusion length of minority charge carriers in GaN nanowires. Since the geometrical symmetry of a nanowire and the role of the surface is vastly different from that of bulk materials, measuring the diffusion length is an important step in the characterization process.

The second objective is to provide independent verification of the accuracy of the unique optical characterization technique developed at the Naval Postgraduate School (NPS) [3–5]. This special transport imaging technique combines Atomic Force Microscopy (AFM), Near-field Scanning Optical Microscopy (NSOM), and Scanning Electron Microscopy (SEM) to map luminescence produced by diffused minority charge carriers by retaining the spatial information. By using the widely utilized Electron Beam Induced Current (EBIC) method, which is traditionally used for the characterization of charge carriers in bulk materials or planar structures, the correlated results can serve as a validation of both techniques.

C. MILITARY RELEVANCE

Nanotechnology is an opportunity for another breakthrough in defense evolution. Nanotechnology has a wide range of potential defense applications in the fields of sensors, nanorobotics, nanoelectronics, propellants, explosives and to enhance the performance of devices and weapon systems [6]. In all these areas, nanotechnology holds two great promises in that it allows for the miniaturization of existing equipment, making soldiering equipment smaller,

lighter and more concealable and it allows the development of new materials such as the new armor for the M1A1 Abrams tanks that increases survivability [7–8].

D. THESIS OVERVIEW

This thesis begins with a brief introduction of nanotechnology, its importance and its military relevance. Chapter II provides the background on minority charge carriers, focusing on the generation and motion of these charge carriers in semiconductor structures. This chapter also presents a general background on diffusion length and how charge carriers diffuse in nanostructures.

Chapter III covers the literature review on the two different methods of measuring diffusion lengths used at NPS. The chapter explains the use of the EBIC method compared to the NSOM method and explores each method's pros, cons and challenges.

Chapter IV describes the experimental equipment and approach for the EBIC measurements. It introduces the equipment used in these experiments and the basic parameters of the experiments. The chapter describes the characteristics of each nanowire sample in detail and the procedure of how data are collected and analyzed.

Chapter V reports the results obtained from the EBIC experiments. It reports on the determination of the diffusion length for each wire sample.

Finally, chapter VI presents the final analyzed diffusion lengths. This chapter also discusses the outstanding questions regarding the EBIC results obtained from the various samples and presents suggestions for future research. The thesis concludes by assessing whether the thesis work has met its stated objectives.

THIS PAGE INTENTIONALLY LEFT BLANK

II. BACKGROUND ON MINORITY CHARGE CARRIERS

All solid materials can be broadly classified into three categories with regard to their electronic properties: metals, insulators, and semiconductors. What distinguishes each group is the material resistivity, or conductivity. Metals are good conductors at any temperature due to the large concentration of free electrons that are readily available for conduction. Insulators are poor conductors as most of the electrons are bound in the valence band under most conditions. Semiconductors are a special class of materials that change their conductivity under different conditions. Figure 1 shows the classification of materials by conductivity. In general, current conduction is due to the drift of mobile charges through a material under an applied electric field. In most metals, the mobile charges are electrons. For non-metals such as semiconductors, there are other types of mobile charge [9], including missing electron states known as positively charged “holes.”

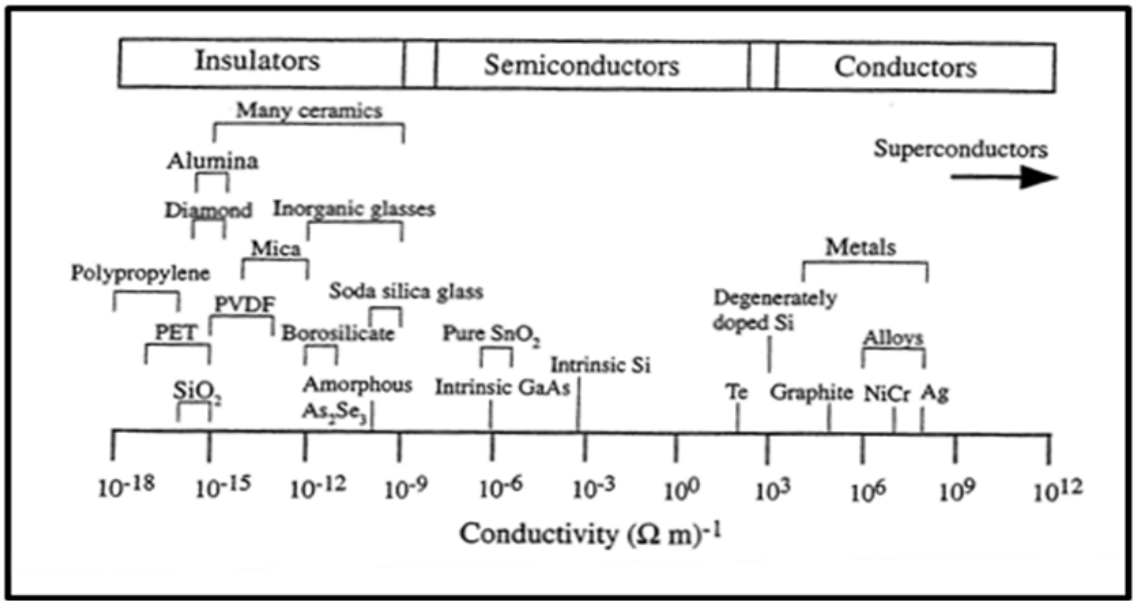

Figure 1. Range of Conductivities Exhibited by Various Materials (From [10])

A. GENERATION OF CHARGE CARRIERS IN SEMICONDUCTORS

Both electrons and holes can participate in the process of conduction in semiconductors. The number of electrons and holes available for conduction is dependent on the temperature and concentration of dopants. At low temperature, almost all of the electrons are bounded in the valence band and there are minimal electrons in the conduction band, resulting in low electrical conductivity. When the temperature is increased, the thermal energy present will result in the excitation of electrons from the valence band to the conduction band. For a semiconductor in thermal equilibrium, the intrinsic carrier concentration, n_i, can be determined by the equation:

$$np = n_i^2 = N_c N_v \exp\left(-\frac{E_g}{kT}\right) \tag{2.1}$$

where E_g is the bandgap energy of the semiconductor material, k is the Boltzmann's constant, T is the temperature of the material, and N_c is a temperature-dependent constant called the effective density of states at conduction band edge given by:

$$N_c = 2\left(\frac{2\pi m_e^* kT}{h^2}\right)^{\frac{3}{2}} \tag{2.2}$$

and N_v is a temperature-dependent constant called the effective density of states at valence band edge given by:

$$N_v = 2\left(\frac{2\pi m_h^* kT}{h^2}\right)^{\frac{3}{2}} \tag{2.3}$$

where m_e^* and m_h^* are the effective mass of electrons and holes respectively and k is Planck's constant.

If the semiconductor is doped, then the concentration of electrons and holes can be found by:

$$n = \left(N_d - N_a\right) \tag{2.4}$$

and

$$p = \frac{n_i^2}{\left(N_d - N_a\right)} \tag{2.5}$$

for n-type semiconductors and

$$p = \left(N_a - N_d\right) \tag{2.6}$$

and

$$n = \frac{n_i^2}{\left(N_a - N_d\right)} \tag{2.7}$$

for p-type semiconductors, where N_a is the concentration of acceptors and N_d is the concentration of donors.

Therefore the creation of electron-hole pairs in an n-type semiconductor will have a larger impact on the value of p than the value of n. Similarly, generation of electron-hole pairs in a p-type semiconductor will have more impact on the electron concentration than on the hole concentration. Thus, the electrical properties of semiconductors under external excitation are often determined by the minority charge carriers.

Other than thermal excitation, electrons can be excited into the valence band by sources such as an external electric field, incident photons with energies larger than the material's bandgap, means of chemical reaction and even excitation by acoustics. In this thesis, excitation is done by an incident high energy electron beam in a scanning electron microscope. These highly energetic electrons will interact with valence electrons in the material to produce electrons that have enough energy to go into the conduction band and leave behind holes in the valence band. This process is summarized in Figure 2.

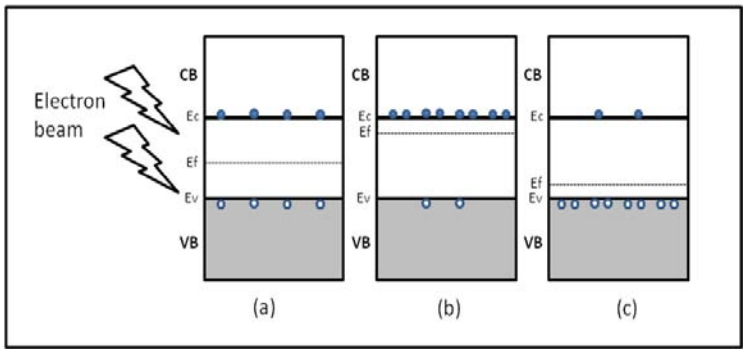

Figure 2. Energy Band and Relative Concentration of Electrons and Holes for (a) Intrinsic, (b) n-Type, and (c) p-Type Semiconductors

B. MOVEMENT OF MINORITY CHARGE CARRIERS

In order to understand how the generated charge carriers move within the semiconductor, it is important to understand the structure of the energy bands. While there are at least 67 major semiconductor devices with over 100 variations identified [11], all of these devices are founded on a much smaller number of building blocks. Highly complex devices, such as transistors, lasers and optical detectors, are made from combinations of these fundamental components. Figure 3 summarizes these building blocks.

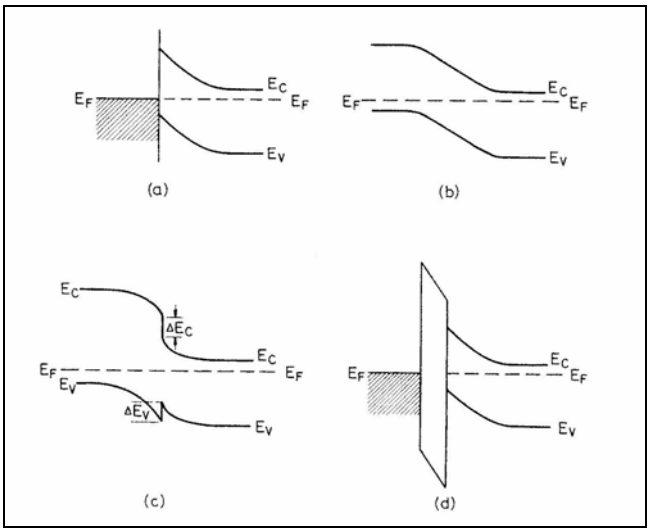

Figure 3. Basic Building Blocks of Semiconductor Devices—(a) Metal-Semiconductor Interface, (b) p-n Junction, (c) Heterojunction Interface, and (d) MOS Structure (From [12])

Semiconductor devices thus have the unique property of being able to control charge carrier populations by utilizing the internal and external fields present at various interfaces. By exploiting the difference in energy across each of the boundaries shown in Figure 3, an internal field is created because charge carriers move to regions of lower potential energy to achieve higher stability. By applying an external field, i.e., forward or reverse bias, the charge carrier population can either be enhanced or depleted. This is unlike metals, where charge carriers are always present in abundance and an external field would simply move the charge carriers faster. In order to control and study the current in nanostructures, contacts must be made. The critical technology challenge is thus to make contacts to the nanowire as the contact controls both conductivity and the ability to make devices. In addition, the contacts allow connection to the outside world and thus make the nanowires a potential commercial technology.

The metal-semiconductor interface is of great interest in this thesis because collecting the EBIC signal requires the nanowire sample to be connected to an external circuit. The metal-semiconductor interface is also the means of introducing internal fields, as shown in Figure 3. This connection is made possible by depositing thin films of metal which, act as probes on the semiconductor devices. Details of how the samples are prepared are discussed in Chapter IV. Figure 4 shows a typical metal-semiconductor connection made on a nanowire sample that is prepared for EBIC.

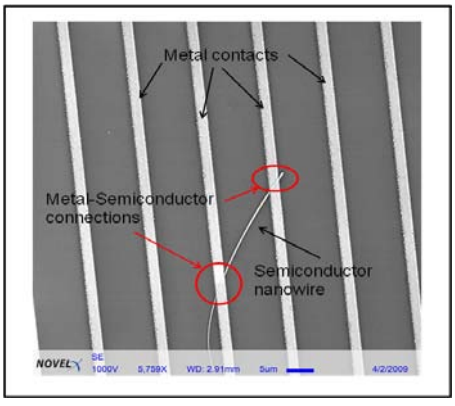

Figure 4. SEM Image of Metal-Semiconductor Contact to GaN Nanowire Taken at 5,700x Magnification

Consider the n-type metal-semiconductor contact as an example. When an electron-hole pair is generated in the vicinity of the barrier, the minority charge carrier, hole, will move under the influence of the electric field toward the metal contact given that that is the path of decreased energy. The electron will travel away from the metal contact given the presence of the same internal potential barrier. The reverse is true for the case of electrons drifting towards the metal and holes moving away from the metal in a p-type semiconductor. Figure 5 shows the movement of the charge carriers under zero bias condition, meaning no additional applied electric fields.

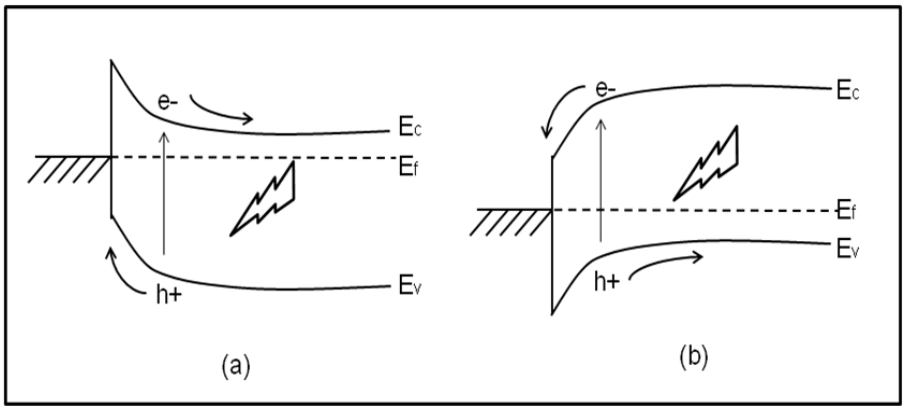

Figure 5. Movement of Charge Carriers Under Zero Bias Condition for (a) n-Type and (b) p-Type Metal-Semiconductor Contacts

When an external bias is present, the energy barrier is affected by the magnitude of the bias as illustrated in Figure 6. The reduced barrier under forward bias is the mechanism for switching in diodes and transistors. In EBIC, we study current flow under external excitation and zero bias condition to understand material properties in the region adjacent to the metal interface.

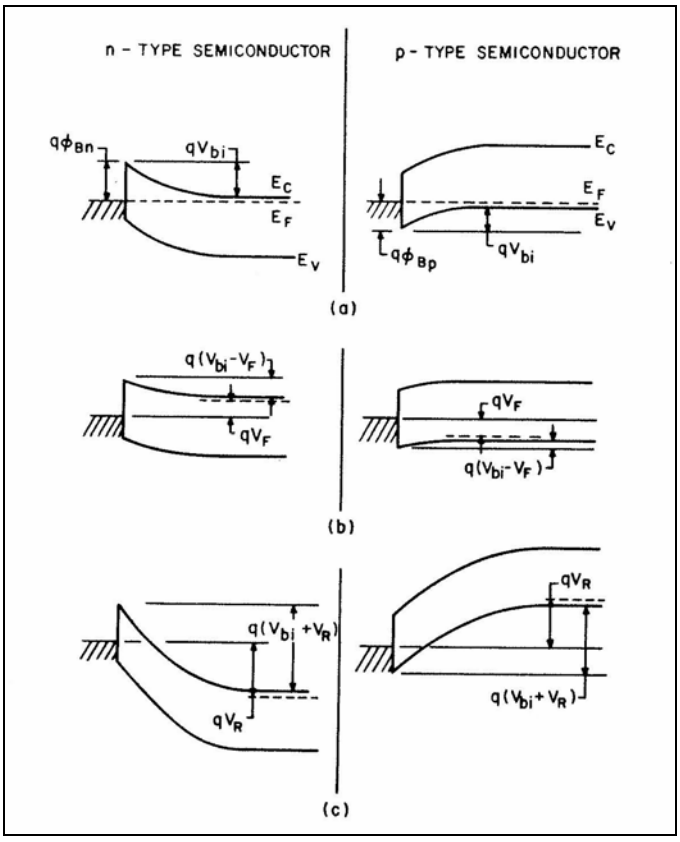

Figure 6. Energy Band Diagram of Metal-Semiconductor (n-Type and p-Type) Under Different Bias—(a) Thermal Equilibrium, (B) Forward Bias, and (C) Reverse Bias (From [13])

C. DIFFUSION LENGTH

Free charge carriers in semiconductors move with two different but related phenomenon: drift and diffusion. When the semiconductor is subjected to an applied electric field, E, the charge, q, will experience a force qE. Apart from the velocity that the charge has acquired from thermal energy, this additional force will give the charge an added net velocity in the direction of the field. This field-dependent velocity is, therefore, called drift velocity [13].

If we consider conservation of momentum, the net momentum on the charge can then be expressed as:

$$qE\tau_c = mv_d \tag{2.8}$$

where τ_c is the lifetime of the charge and v_d is the drift velocity of the charge carrier. Re-arranging Equation (2.8) gives:

$$v_d = \left(\frac{q\tau_c}{m} \right) E = \mu E \tag{2.9}$$

The parameter μ is called the drift mobility. It describes the ease of movement of a charge carrier in the presence of an applied electric field.

Similarly, diffusion can be regarded as the process through which particles move from a region of high concentration to a region of lower concentration, parallel to charge carrier moving from high potential to low potential in an E-field. Using Einstein's relation, the diffusion coefficient, D, and drift mobility, μ, are linked via the relation

$$D = \frac{kT\mu}{q} \tag{2.10}$$

Since current is a measure of moving charge particles, current density is related to drift mobility by

$$I_{net} = nq\mu_p E + pq\mu_n E \tag{2.11}$$

where μ_p is the drift mobility of holes, μ_n is the drift mobility of electrons, p is the concentration of holes and n is the concentration of electrons. EBIC measures the diffusion behavior in the region just beyond the depletion field associated with the metal-semiconductor barrier.

One of the goals of this thesis is to measure the average diffusion length of the minority charge carriers in GaN nanowires. This diffusion length is given by the following equation:

$$L_{diff} = \sqrt{D\tau} = \sqrt{\frac{\mu\tau kT}{q}} \tag{2.12}$$

where τ is the lifetime of the minority charge carrier.

D. CHARGE CARRIERS IN NANOSTRUCTURES

What distinguishes nanostructures from bulk materials is that at least one of the physical dimensions must be in the nanoscale [2]. Because of this small dimension, the movement of charge carriers in nanostructures is also different from that of structures with other bigger dimensions. Consider the example of the diffusion of charged particles. In bulk materials in which the arbitrary dimensions in directions x, y and z are large compared to the diffusion length, diffusion is possible in 3-D. If the particle is confined to a region like a thin plane, then diffusion is only possible in directions x and y. Finally, if charge carriers are confined in a space like that of a nanowire, diffusion is confined to 1-D. Figure 7 illustrates the modeling of diffusion of charge carriers in structures of different dimensions.

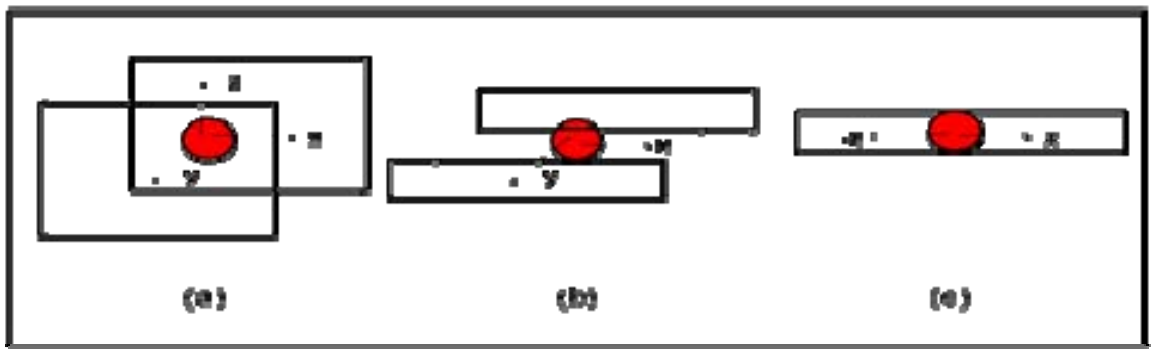

Figure 7. Degrees of Freedom for Diffusion in a (a) Thick Structure, (b) Thin Plane, and (c) Wire

The diffusion current in the far-field for each scenario described in Figure 7 has the spatial dependence shown in Table 1.

Table 1. Diffusion Current in 3-D, 2-D and 1-D

3D	$I \sim \frac{1}{r} e^{-\frac{r}{L_d}}$, where $r = \sqrt{x^2 + y^2 + z^2}$
2D	$I \sim \frac{1}{\sqrt{r}} e^{-\frac{r}{L_d}}$, where $r = \sqrt{x^2 + y^2}$
1D	$I \sim e^{-\frac{r}{L_d}}$, where $r = x$

In this thesis, it is assumed that charge carriers are confined to the nanowire and diffusion can only occur in one direction (i.e., along the wire). Thus the current associated with carrier diffusion from a point source at distance x from the contact along the wire is modeled to be:

$$I \sim I_o e^{-\frac{x}{L_d}} - I_{bc} \tag{2.13}$$

where I_o is the maximum current collected, I_{bc} is the background current, x is the distance and L_d is the diffusion length of the minority charge carriers.

III. METHODS OF MEASURING MINORITY CHARGE CARRIERS DIFUSION LENGTH

A. ELECTRON BEAM INDUCED CURRENT (EBIC)

The Scanning Electron Microscope (SEM) is an instrument that is widely used in the electronics industry to examine the surface features of a sample. An electron beam is generated in the SEM using a cathode-ray tube. The intensity of the beam and its scan pattern can both be controlled, thus enabling a technique called Electron Beam Induced Current (EBIC) that is widely used in the study of electrical defects and to determine the minority-carrier lifetime, τ, and diffusion length, L_d, in semiconductor materials [14].

There are two basic configurations to connect the sample electrically in the SEM, determined by the purpose of the experiment. When doing defect imaging studies, the electron beam is usually incident perpendicular to the collection junction. (Figure 8(a)). In diffusion length measurements, the electron beam is incident parallel to the collection plane [15]. (Figure 8(b)). This thesis concentrates on the measurement of diffusion length, and thus the configuration in Figure 8(b) will be used and discussed.

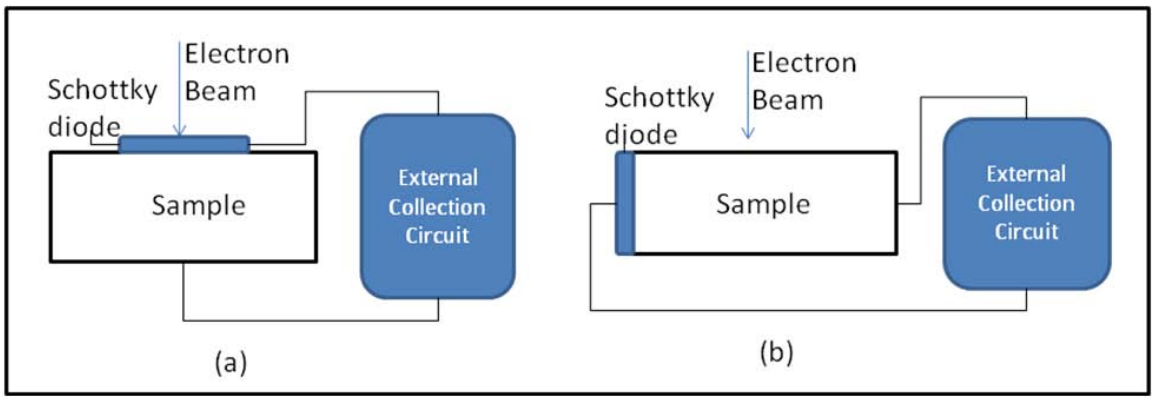

Figure 8. EBIC Configurations for (a) Defect Imaging with the Electron Beam Parallel to the Metal Interface and (b) Diffusion Length Measurement with the Electron Beam Perpendicular to the Metal Interface

The principle behind EBIC is relatively straightforward. When a beam of highly energetic electrons is incident onto a semiconductor sample, in this case a semiconductor nanowire, electron-hole pairs are formed. The generation factor (i.e., number of electron hole pairs generated per incident beam electron) is determined by the following equation:

$$G = \frac{E_b(1-\gamma)}{E_i} \tag{2.14}$$

where E_b is the electron beam energy, E_i is the ionization energy of the material, and γ is the fractional electron beam energy loss due to the backscattered electrons [16].

Figure 9 shows that the ionization energy for GaN (E_g ~3.4 eV) is about 11 eV. Therefore, the generation factor, G, for GaN in the case when there is no energy loss due to backscattering (i.e., γ = 0) is approximately 1,800. In other words, for every incident beam electron, 1,800 electron-hole pairs will be generated in the nanowire. With this gain effect, it can be assumed that the current collected in EBIC is generated by the wire and not by the initial electron beam from the SEM.

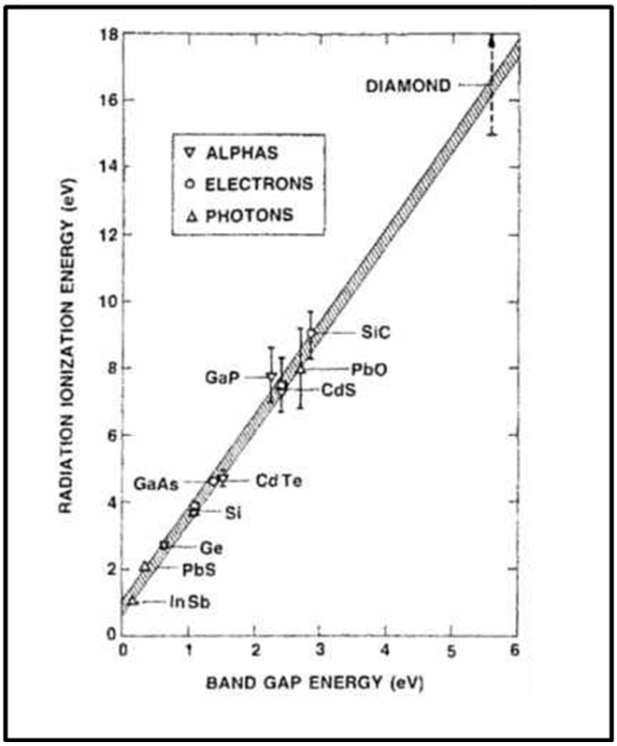

Figure 9. The Effective Ionization Energy (i.e., the Average Energy Required for the Generation of an Electron-Hole Pair) for Incident Radiation as a Function of the Band-Gap Energy E_g (From [16])

Depending on the doping level of the sample, there is a population of majority carriers and minority carriers. If we take the case of an n-type semiconductor as an example, the majority carriers are electrons. Under normal equilibrium conditions, these electrons will diffuse in order to achieve electrical neutrality in the sample. When the sample is excited by an external electron beam, excess electron-hole pairs are generated. Since the excess electron density is smaller than the equilibrium density, the excess electrons will follow the diffusive motion of the injected minority carriers in order to insure that charge neutrality is maintained [17]. As indicated in Chapter II, there may be an internal field created at the metal-semiconductor interface; this field will act on the minority charge carriers causing a net current flow. Thus, EBIC is, in simple terms, a measurement of this current generated when a semiconductor sample is excited by an external electron source.

This additional current collected is related to diffusion length of the minority charge carrier by the following equation:

$$I \sim I_o e^{\frac{-x}{L_d}} \tag{2.15}$$

where I_0 is the maximum current, x is the distance of electron beam from the collection junction and L_d is the minority charge carrier diffusion length. This equation assumes that current is restricted to flow in a 1-D space, which, in this case, is along the wire, as discussed in the previous chapter.

B. NEAR FIELD SCANNING OPTICAL MICROSCOPY (NSOM)

Near Field Scanning Optical Microscopy (NSOM), as the name suggests, uses light to map the properties of a sample. Traditional optical microscopy is limited by diffraction and thus the resolution is restricted. The diffraction limit is described by

$$d > \frac{\lambda}{2\sin\theta} \tag{2.16}$$

where d is the distance between two objects, λ is the wavelength of light, and θ is the angle through which light is collected. Under visible light, the highest resolution (i.e., smallest d) achievable by the traditional optical microscopy system is 200 nm. This is achieved by using the shortest wavelength for visible light, 400 nm, and choosing θ to be 90°. Traditional optical microscopy is also known as Far-Field Scanning Optical Microscopy (FSOM) because diffraction effects dominate for collection in the “far-field,” i.e., collection at distances greater than several wavelengths from the sample.

To do NSOM, the light source and the collection tip should ideally be within one wavelength from the surface that is to be scanned. Similar to AFM, the feedback mechanism will keep the distance between the tip and the sample constant. The light source is then scanned across the surface of interest and any optical signal resulting from reflection or luminescence is collected [18].

At NPS, a special setup is used to do NSOM. Instead of using a point light source as the excitation source, the SEM is used. As in EBIC, a highly energetic beam of electrons is used to create electron-hole pairs in the semiconductor sample. In the absence of an electric field, two processes will then take place after the generation of the electron-hole pair: diffusion and recombination. The extent of diffusion is determined by the concentration of the excess charge carriers, surface of the material and the existence of defects. The rate of recombination is determined by the material properties. During recombination, photons of wavelength related to the energy band of the semiconductor device will be emitted. Thus, by measuring the location and intensity of the emitted photons, the diffusion length of the minority charge carrier in the semiconductor device can be measured. Figure 10 shows the setup of the SEM-NSOM used at NPS.

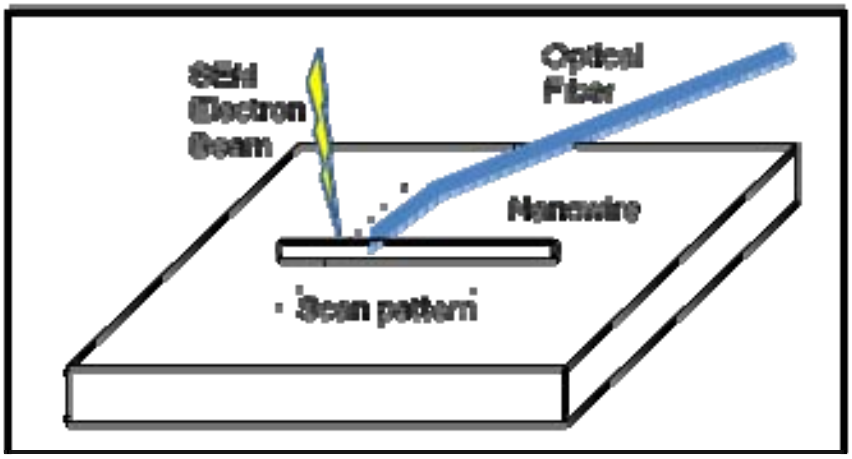

Figure 10. SEM-NSOM Setup Showing the SEM Electron Beam Exciting the Nanowire Sample and the Optical Fiber Tip Scanning the Surface of the Nanowire while Collecting Photons Emitted from the Recombination Process

C. EBIC VERSUS NSOM

The fact that both EBIC and NSOM are capable of measuring minority charge carrier diffusion length allows a parallel and independent verification to be made. While this thesis uses EBIC to find the diffusion length, another student,

LCDR Lee Baird, is working on using NSOM to find the minority charge carrier diffusion length. One goal of this thesis is to take independent measurements of L_d in GaN nanowires since very few measurements exist to date. This will provide new materials data and allow evaluation of the new NSOM approach as well as identify the advantages and challenges of EBIC for nanoscale devices.

The advantages and challenges of employing EBIC in the study of the minority charge carriers are as follows.

1. Need to Make Connection to Small Features

The first challenge to performing EBIC on nanowires is the need to make metallic contact to the nanowires so that external circuitry can be connected. Since it is very difficult to install and operate a probe station in the SEM, metal grids are usually deposited onto the substrate containing the nanowire using optical lithography, and, through selective etching, contacts can be made on the nanowire. After this, contacts from the metal grids to the external circuits can then be made by means of wire bonding. This process is both time consuming and prone to errors, as the nanowire could be destroyed in the process.

2. Non Intrusive Method

Other than making the metal contact to the sample being studied, EBIC is generally a non-intrusive method. Given that the energy of the electron beam in the SEM is low (0.1 to 40 keV for JEOL 840A), it is not enough to cause any structural damage to the sample. While EBIC is good for the study of bulk materials, it can be a challenge to create the desired contacts on nanostructures. Due to the size of nanowires, making metal contacts is more probabilistic than deterministic. Developments in metal deposition such as electron beam lithography and optical lithography have progressed to allow operators to customize the areas to make the contacts, making the process of contact making slightly easier and faster. After the metal contacts have been made, EBIC is subsequently a “non-contact” technique. Other than the electron beam hitting the

sample and electrons and holes moving within the material, everything else is driven and collected externally. This is a major advantage of EBIC because it preserves the sample for further experimental opportunities.

3. Need for Ohmic Contact

Ideal EBIC is performed with a Schottky-Ohmic contact pair. Traditionally, EBIC is done on bulk and film materials whereby the contact pairs are far apart compared with the area of interest. Thus, even if both the contacts are Schottky, it can be assumed that a Schottky-Ohmic contact pair still exists given the large inter-contact distance. However, in the case of nanowires, the length of the wire might be only a couple of diffusion lengths long. With such short lengths, the two contacts cannot be assumed to be far apart. The structure is now more like two overlapping contact regions. Furthermore, it has proven so far to be technically challenging to make an ohmic contact with metal deposition to GaN nanowires [19], as the metal-semiconductor contact will have to go through an annealing process after lithography.

4. Fast and Repeatable Experiments

An advantage of EBIC is that experiments are relatively fast and repeatable if the parameters are kept constant. This thesis shows that results are very reproducible but are affected by the amount of background noise that is present during each experiment and the stability of the electron beam and the sample stage. Given the small magnitude of current (~1x10-4 μA) that we are trying to measure, noise (e.g., stray and background current) can be significant. Also given the size of nanowire (diameter of 100-300 nm) compared with the size of the electron beam (diameter of 50 nm), the position at which the electron beam hits the sample becomes critical. Any small vibrations to the SEM will result in the electron beam wandering off the sample and giving false signals.

Table 2 shows the relation between probe current and beam diameter for our JEOL 840A.

Table 2. Probe Current Versus Beam Diameter for 30 keV SEM Beam (From [20])

Probe current (A)	16% - 84%(2σ) (nm)	FWHM (nm)
$1x10^{-11}$	34	40
$3x10^{-11}$	39	46
$1x10^{-10}$	48	56
$3x10^{-10}$	107	126
$1x10^{-9}$	139	163

In order to illustrate the effect of electron beam "drifting" due to vibrations and movement of the stage, a simple control experiment was conducted. In this experiment, the electron beam is made to repeatedly scan a particular line over a nanowire as shown in Figure 11.

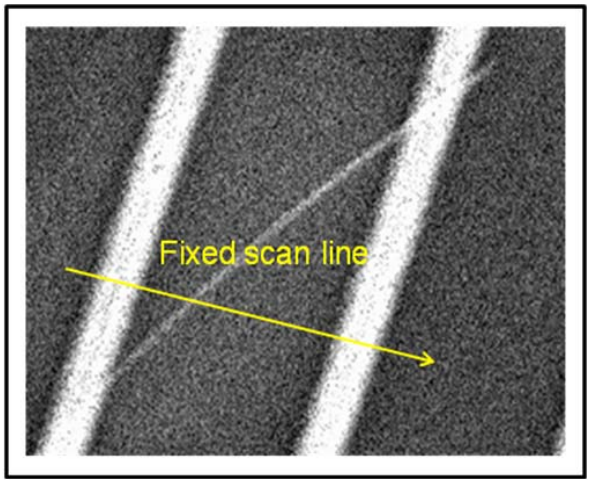

Figure 11. Fixed Scan Line to Investigate Drifting of Electron Beam on Nanowire: Image is Taken at 6,000x Magnification

Signal is collected at different vibration levels, determined by the water pump, and illustrates the effect external vibrations have on the stability of the electron beam. Figure 12(a) shows the EBIC signal during multiple scans when the water pump is at low vibration level. Since the line scan routine is fixed, the peak in the signals corresponds to the center of the nanowire when the electron

beam is directly incident. Figure 12(b) shows a magnified view of the peaks of the EBIC signal over a range of 0.6 μm to see the variation in the position of the nanowire during the multiple scans. Similarly, Figure 13 shows the position of the electron beam when the water pump is at high vibration level and Figure 14 shows the position of the electron beam when the water pump transits from low to high vibration level.

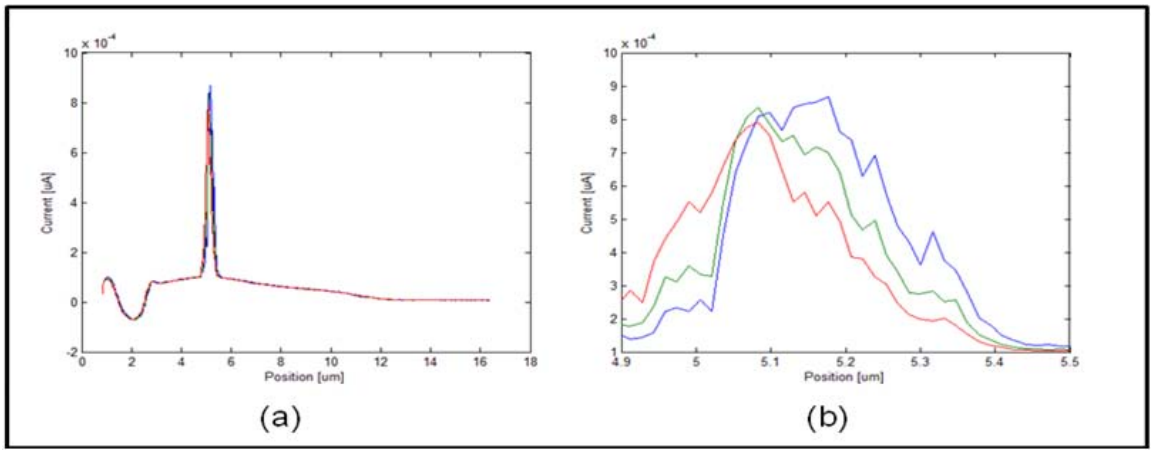

Figure 12. EBIC Signal as a Function of the Electron Beam Position When Water Pump is at Low Vibration Level—(a) Nanowire Seemed to be on the Same Spot at Macro-View and, (b) Deviation Of Position of Nanowire on Expanded Scale ($\Delta x = 0.6\mu m$)

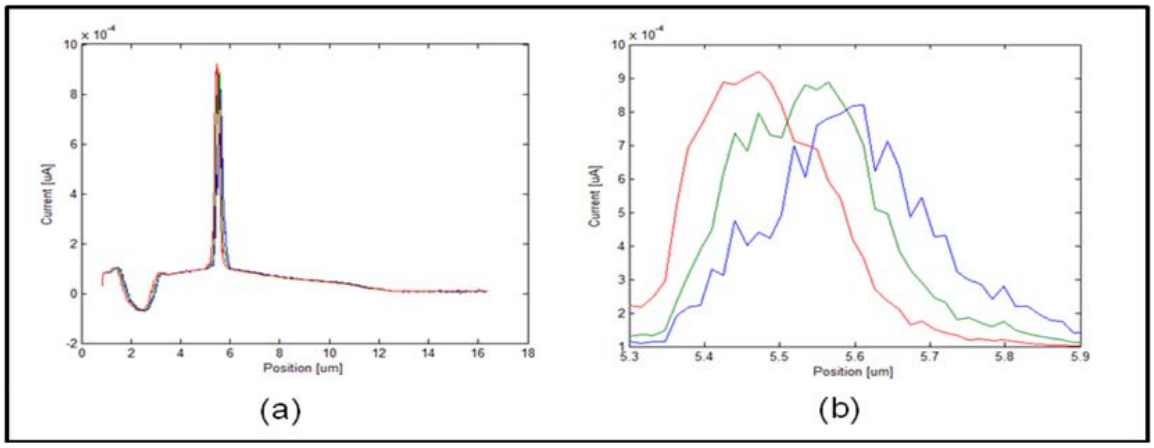

Figure 13. EBIC Signal as a Function of the Electron Beam Position when Water Pump is at High Vibration Level—(a) Nanowire Seemed to be on the Same Spot at Macro-View and, (b) Deviation of Position of Nanowire on Expanded Scale ($\Delta x = 0.6\mu m$)

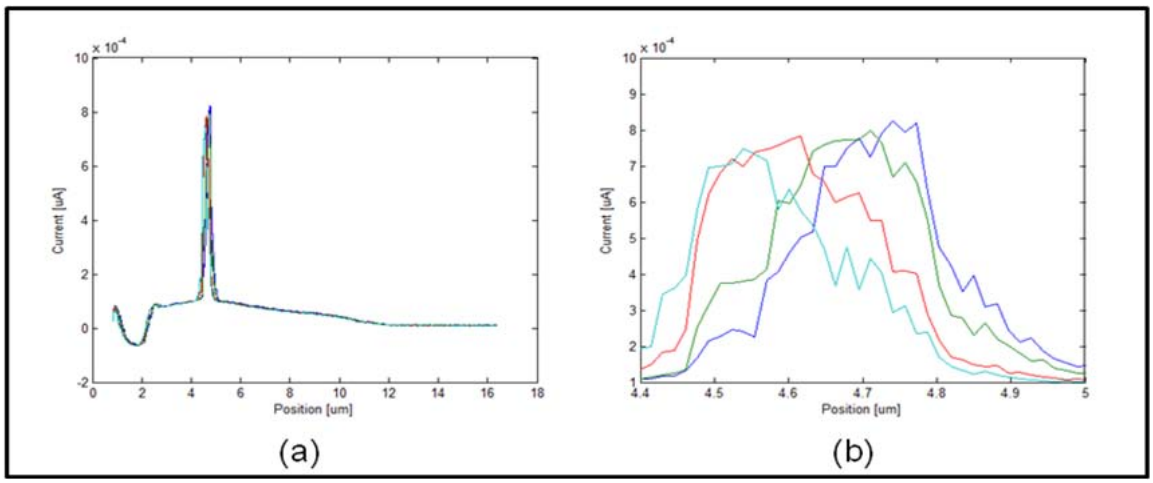

Figure 14. EBIC Signal as a Function of the Electron Beam Position when Water Pump Transits from Low to High Vibration Level—(a) Nanowire Seemed to be on the Same Spot at Macro-View and, (b) Deviation of Position of Nanowire on Expanded Scale ($\Delta x = 0.6\mu m$)

From Figures 12b, 13b and 14b, the average drift of the electron beam is found to be 94 nm, 123 nm and 148 nm respectively. Compared with the beam width of 50 nm at 20 kV, the drift can be as large as three lateral widths. These results not only confirm that the position of the electron beam on the sample is very sensitive to vibrations; they demonstrate that diffusion length has to be extracted from area scans instead of single line scans so the vibration effects can be averaged.

D. ADVANTAGES AND CHALLENGES OF NSOM

The advantages and challenges of using NSOM to measure minority charge carriers are as follows.

1. Calibration Needed

While NSOM is also potentially a non-intrusive technique, the resolution is dependent on the collecting tip being in very close proximity to the sample surface. With this requirement, it is imperative to calibrate the NSOM for each sample that is to be examined. This process, thus far, is mostly trial-and-error based. At the bulk material level, calibration is relatively easy. However, at nano-

scale, calibration requires the operator to be both skilled and experienced. If the operator is not skilled, nor experienced, the nanowire can break when NSOM tip scans across the wire.

2. Bandgap Dependent

Since NSOM measures the photon that is re-emitted from electron-hole pair recombination, it is bandgap dependent. This means that not all materials may be suitable to be examined using NSOM. In general, materials with direct bandgaps produce significantly more luminescence and are more suitable for NSOM. In addition the results from NSOM are dependent on the geometry of the sample. If light is emitted in any other direction other than toward the NSOM tip, signal can be lost.

3. Relatively Long Experiment Runs

Similar to EBIC, NSOM experiments are easily reproducible. The only difference is the time taken for each experiment. Compared with EBIC, the time needed to run a single scan in NSOM is much longer. This timing increases if high-resolution images are desired. The advantage of NSOM over EBIC will then be the time needed to interpret the data. Unlike EBIC, the advantage for running NSOM is that diffusion length can be extracted relatively easily from the data collected, and no collecting contact is required.

THIS PAGE INTENTIONALLY LEFT BLANK

IV. EXPERIMENTAL SETUP AND PROCEDURE

A. THE SCANNING ELECTRON MICROSCOPE (SEM)

The SEM used for this thesis work is a JEOL 840A SEM. It is comprised of two major components—the Electron Column and the Control Console. See Figure 15. The electron column consists of a thermionic emission electron gun, several magnetic lenses that control the path and focus of the electron beam and an evacuated chamber that is capable of maintaining pressure at ~10^{-4} to 10^{-5} Pa [21].

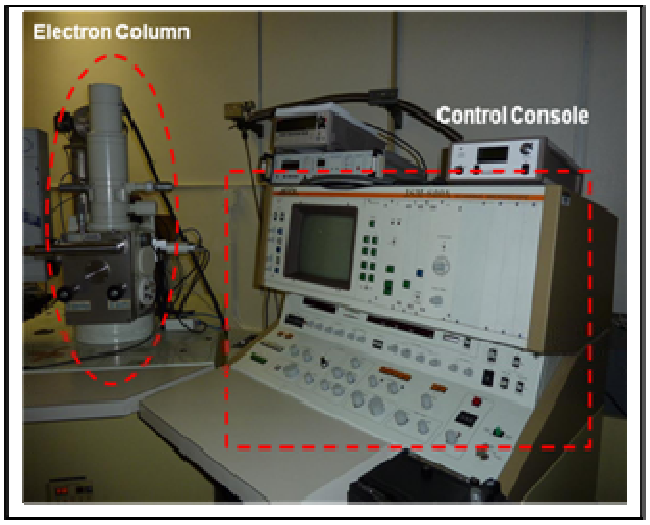

Figure 15. JEOL 840A SEM

The electron gun produces an electron beam by heating up a tungsten filament to a range of 2,000–2,700 K. The electrons are then accelerated to energies in the range of 0.1–40 keV via controls on the control console. The intensity of the beam is controlled by the probe current which is in the range of $6x10^{-12}$ A to $6x10^{-8}$ A. The spot size of the electron beam is less than 10 nm at the lowest probe current (see Chapter III) and the penetration depth of the electron beam ranges from 1–10 µm depending on the beam energy and the material being investigated. The JEOL 840A has a magnification range of up to 300,000x.

By passing the electrons through a series of deflection coils, the SEM is able to steer and scan the electron beam across the surface of a sample and thus create an image. A scan generator is used to generate both the scan pattern for the electron beam and the raster on the control panel for the operator to view. The scan generator moves the electron beam to designated locations along a line to produce a line scan and an area scan is produced by combining many parallel line scans [21].

The sample is mounted on a stage and connected to the BNC connectors as shown in Figure 16. For EBIC measurement, the BNCs are then connected to an external current amplifier shown in Figure 17. The signal generated will then be read by the amplifier and collected by the Oxford Instrument Cathodoluminescence (CL)/EBIC System Software for further analysis.

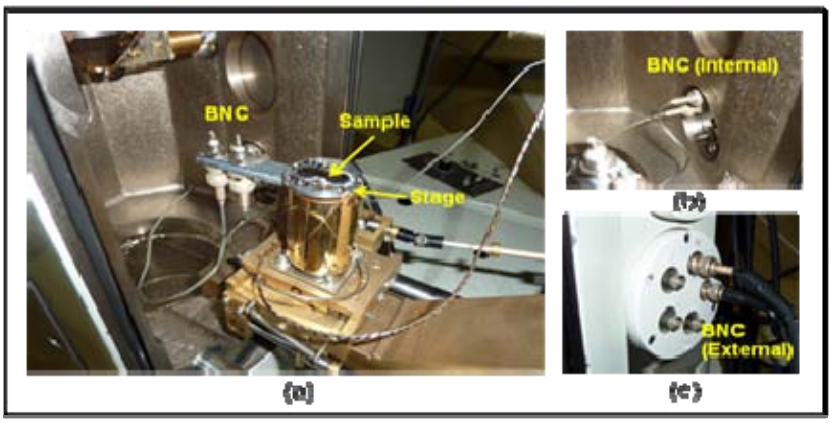

Figure 16. Mounted Sample in SEM

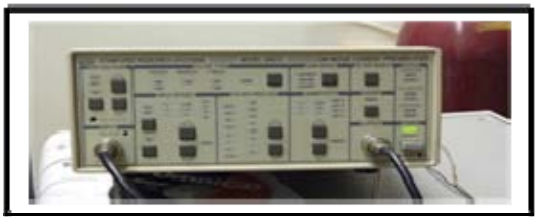

Figure 17. Low Noise Current Amplifier

B. NANOWIRE SAMPLES

Three sets of nanowire samples are investigated in the course of this thesis. The first two sets consist of n-type gallium nitride wires coated with a layer of aluminum gallium nitride (Core/Shell: GaN/AlGaN) and the third set consisted of three unintentionally doped uncoated gallium nitride nanowires (GaN). This allowed investigation on the role of the "shell" layer in these "core-shell" nanowire structures. There is great interest in the role of a thin barrier layer on transport properties and surface recombination. All the wires were grown by Dr George Wang and his colleagues at Sandia National Laboratories. Details on how each sample was grown and prepared are as described below.

1. Sample 1: GaN/AlGaN Nanowire

GaN nanowires are primarily grown using the vapor-liquid-solid (VLS) or vapor-solid-solid (VSS) epitaxy method. VLS is a mechanism that grows one dimensional structures—in this case, nanowires—from chemical vapour deposition [22]. In the case of GaN nanowires, gas phase Ga and N precursors are dissolved in a transition metal catalyst—in our case, Ni—and then precipitated on a substrate as single-crystalline nanowires. As a metal catalyst is used, this VLS method is also known as the metal catalyzed metal-organic chemical vapor deposit (MOCVD) method. Once the core GaN nanowire is grown, the AlGaN layer is subsequently grown in situ by dissolving an Al source in a carrier gas. In this case, the Al source is trimethylaluminum and the carrier gas is hydrogen. The result of the two processes is nanowires that are coated with a layer of AlGaN that is about 5 nm thick [23–25].

Figure 18 shows the SEM image of the nanowire. The end-to-end length of wire that is between the metal contacts is measured to be about 14.4 μm. The average thickness is about 800 nm. ImageJ [26] software is used to measure the dimensions of the nanowires. It is an open source Java based image processing and analysis software that can calculate dimensions of features in images based on pixel scaling.

The metal contacts are deposited onto the substrate using optical lithography. A layer of Ni/Au (40 nm / 70 nm) is first deposited on the substrate and electrode patterns are then defined using optical lithography. The excess Ni/Au is then etched away using O_2 plasma and electron beam evaporation and lift off. The results of this lithography are nanowires held in place on the substrate with the Ni/Au electrodes acting as metal probes that allow external circuitry to be connected.

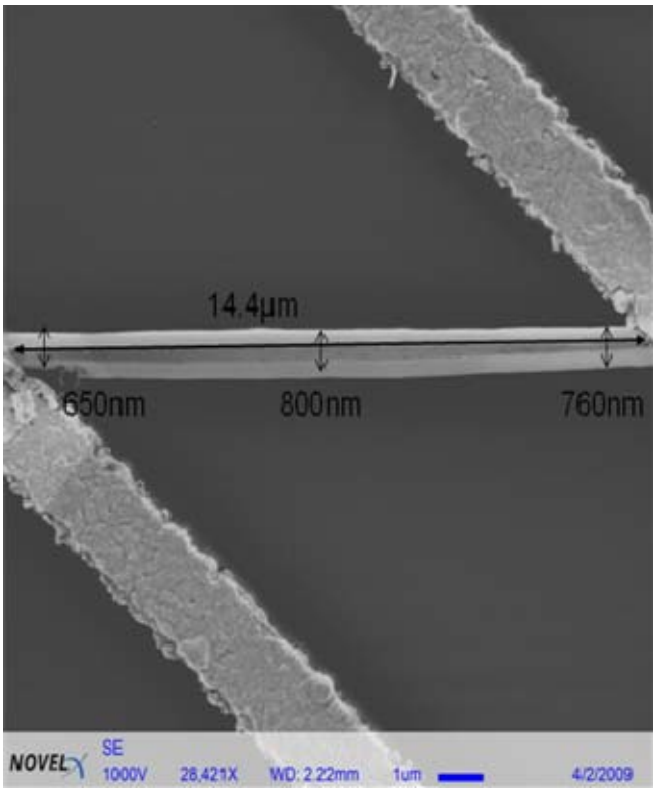

Figure 18. SEM Image of Sample 1—GaN/AlGaN Nanowire, Taken with Electron Beam at 1 kV and 28,000x Magnification

2. Sample 2: GaN/AlGaN Nanowire

Sample 2 is prepared using the same method as that used for Sample 1. The only difference between these two samples is the length and thickness of the wire. Figure 19 shows the SEM image of the nanowire in Sample 2. The end-to-end length of wire that is between the metal contacts measures about 18.7 µm. The average thickness is about 300 nm.

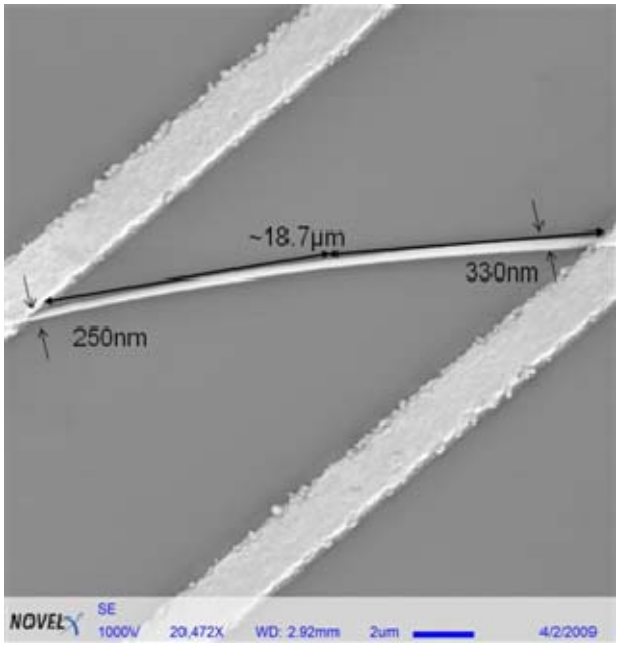

Figure 19. SEM Image of Sample2—AlGaN:GaN Nanowire, Taken with Electron Beam at 1 kV and 20,000x Magnification

3. Sample 3: Uncoated GaN Nanowires

The difference in growth method between Sample 3 and Samples 1 and 2 is the careful control of nanowire growth direction. By aligning the crystallographic growth of the wires on a sapphire substrate, nanowires with more uniform height and diameter can be grown. Also, a Ni catalyst film with submonolayer thickness (1.74 Å) is also used to aid in the aligning of the nanowires [27–29].

Figures 20 and 21 show the two uncoated GaN nanowires in this sample. For Sample 3a, the end-to-end length of wire that is between the metal contacts measures about 1.5 µm. The average thickness is about 230 nm. For Sample 3b, the longest end-to-end length of wire that is between the metal contacts is measured to be about 6 µm. The shorter end-to-end lengths are approximately 1.6 µm each. The average thickness is about 170 nm.

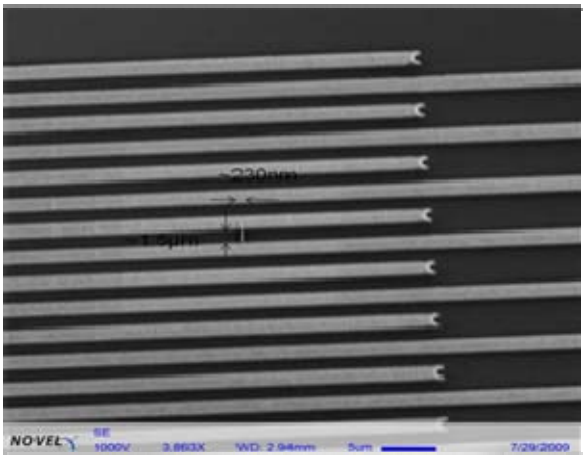

Figure 20. SEM image of Sample 3a—Uncoated GaN nanowire, Taken with Electron Beam at 1 kV and 4,000x Magnification.

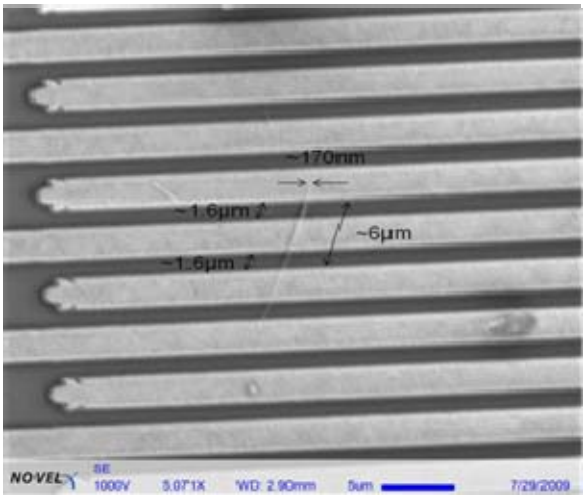

Figure 21. SEM Image of Sample 3b—Uncoated GaN nanowire, Taken with Electron Beam at 1 kV and 5,000x Magnification.

C. DATA COLLECTION PROCEDURE

EBIC can be performed once the sample is connected and loaded, as shown in Figure 16. Two main types of scans are conducted to acquire data from the sample, namely line and area scans. While it is a lot faster to do a line scan, that method faces challenges such as the stability of the electron beam as discussed in Chapter III. Therefore, although the experiment is highly repeatable, the absolute value of the current collected might be different depending on the

exact location of the beam at the designated points. Figure 22 shows an example of a line scan done on Sample 1 and a set of typical current measurements that can be obtained from a line scan. The diffusion length of the material can be extracted from the results shown in Figure 22(b) by doing a regression analysis using Equation 2.13. Figure 22(b) shows that the measured current is positive on one end and negative on the other end.

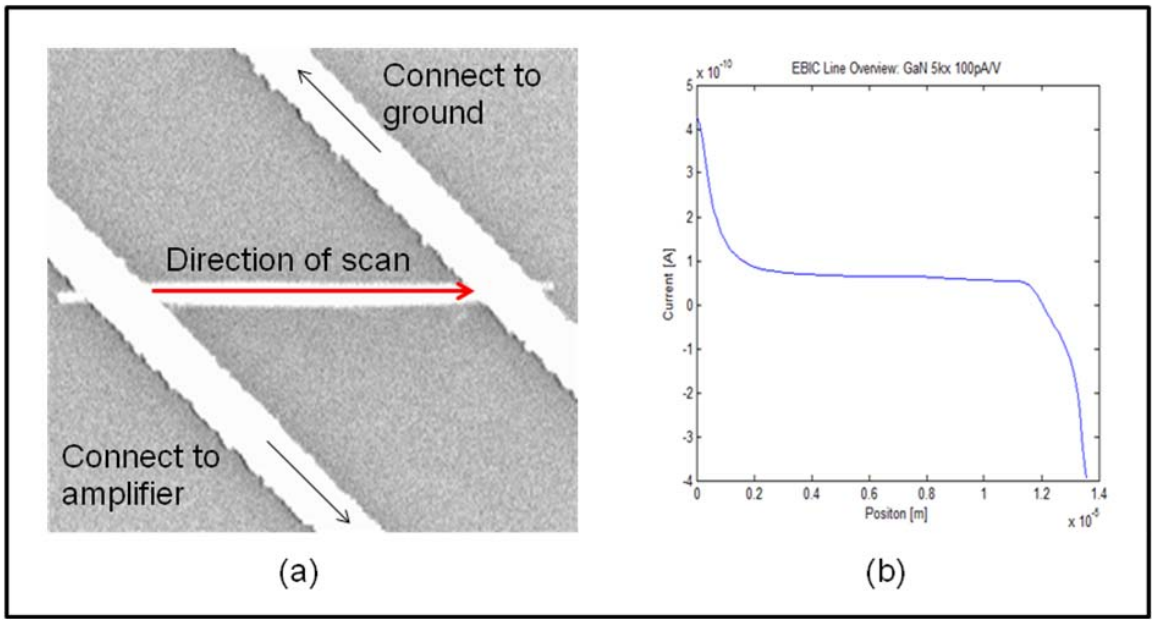

Figure 22. An Example of an EBIC Line Scan—(a) Shows How the Nanowire is Connected to the External Circuitry and the Direction of the EBIC Scan and (b) Shows the Measured EBIC Current from the Line Scan Depicted by Figure 22(a)

Since EBIC is dominated by the minority charge carriers, Figure 22(b) is consistent with the direction of flow of the positive minority charge carriers into the low noise amplifier. To determine whether it is indeed the minority charge carrier that EBIC is measuring, a simple control experiment is conducted. In this experiment, an n-type bulk material—in this case, bulk n-type GaAs with Pt Schottky contact and Au Ohmic contact—is connected to the low noise current amplifier instead of the nanowire. A line scan was performed and the current profile is analyzed. Figure 23 shows the connections and line scan direction of the n-type bulk material and Figure 24 shows the line scan profile obtained from

the experiment. Figure 24 shows that when the electron beam is at the interface between the Pt contact and the n-type GaAs material, the current collected in the amplifier is a positive current. The polarity of the collected current corresponds with the positive current produced by the minority charge carrier, which in this case, is the current produced by the holes.

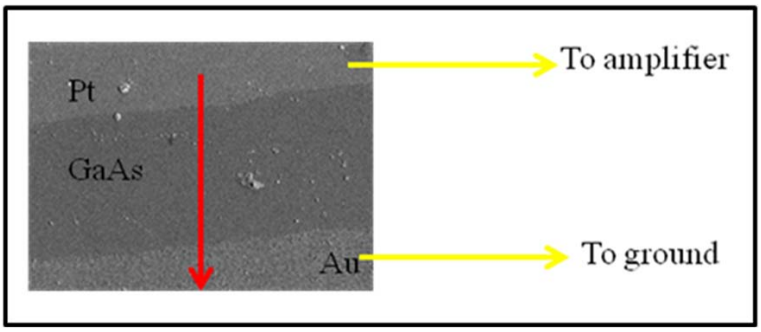

Figure 23. Line Scan (Shown as Red Line) Conducted on Bulk n-Type GaAs Sample

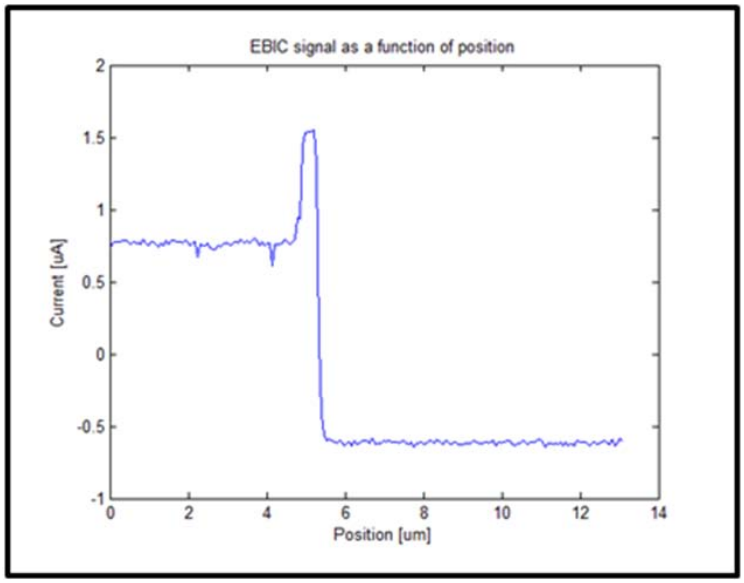

Figure 24. Line Scan Profile of Bulk n-Type GaAs Material (*y*-axis is the Current Measured and *x*-Axis is the Position of Scan)

Figure 25 shows an example of an area scan done on Sample 2 and the data that can be collected from the EBIC system software. While the pictures from the system software offer a good overview of the behavior of the current collected, little can be extracted that is of use to calculate diffusion length. As

such, the data are post-processed in Matlab whereby it is possible to quantify the decay pattern of the current at the contacts and extract the diffusion length.

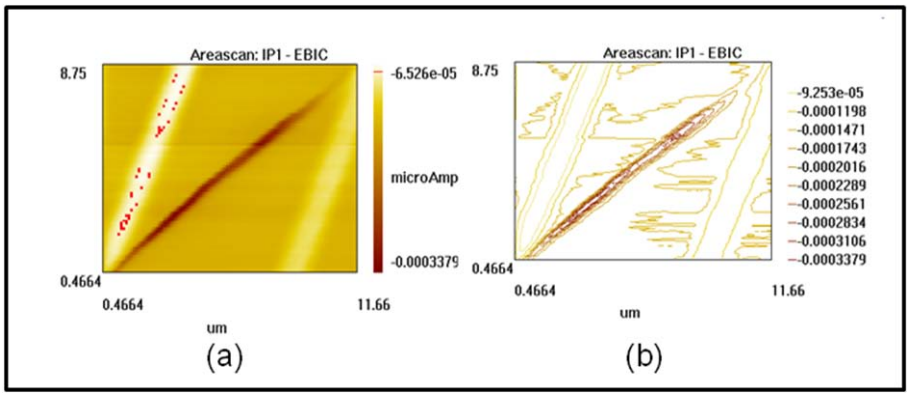

Figure 25. Readout from EBIC System Software—(a) Color Map of the Scanned Area, Intensity of Current Collected is Represented by the Color of Each pixel; and (b) Contour Map of the Scanned Area, Regions of Similar Current Intensity are Connected by a Network of Contour Lines

A three-dimensional image of the data in Figure 25 can be plotted in Matlab using the “Mesh” function. Figure 26 shows the Matlab image. The dark red regions in Figure 26 represent the metallic contacts, which are shown as the whitish area in Figure 25(a), and the bluish signal spanning the two contacts is the nanowire. The amplitude of the bluish signal represents the behavior of EBIC signal.

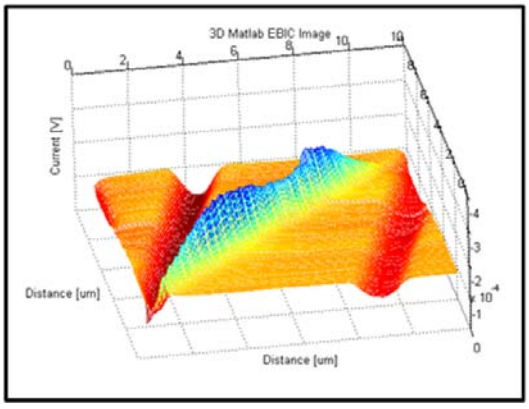

Figure 26. Post-Processed Data using Matlab [Plot of Current intensity (*z*-axis) with Respect to the *x*- and *y*-Positional Axes]

Once the line profile is obtained, the diffusion length can be extracted by doing a linear regression analysis to the current decay as given in Equation 2.13. Matlab functions such as “imagesc” and “improfile” are used to extract the diffusion length. Since these functions are all image processing tools, they calculate the intensity with respect to the pixel of the picture. Therefore, a correlation between the pixel and its actual physical distance on the wire must be performed, so that diffusion length can be expressed as a function of length instead of pixels.

V. DATA ANALYSIS

As discussed in Chapter IV, diffusion length can be extracted either by analyzing the line scan data or the area scan data. This chapter presents the data collected and the calculated diffusion length for each sample.

A. SCHOTTKY CONTACT

Figure 27 shows the I-V characteristic of Sample 2. The sample is connected as shown in Figure 22 and the current generated in the wire is measured as the voltage across the contacts is varied. The non-linear nature of the I-V graph shows that the metal-semiconductor contact is a Schottky contact, and the sample behaves very much like a diode instead of a simple resistor, which would be characterized by a linear graph.

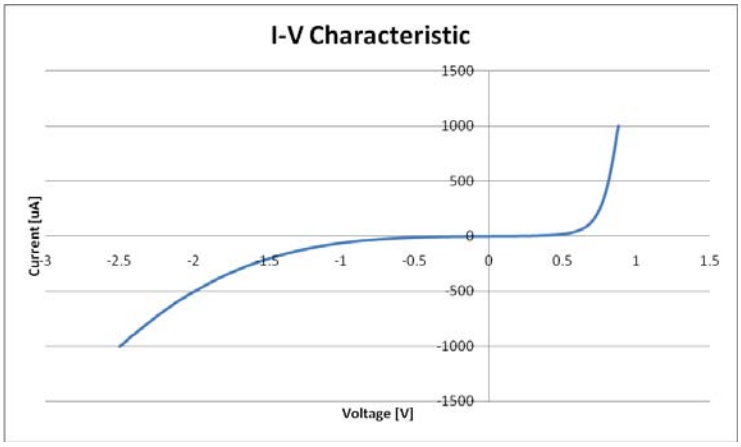

Figure 27. I-V Characteristic of the Metal Contact

B. SAMPLE 1: ALGAN:GAN NANOWIRE

Sample 1 is 14.4 μm long and 800 nm in wide. Due to its thickness, it is possible to extract the diffusion length from both the line and area scans. There are two contacts made to this wire and they are referred to as the left and right contacts. Figure 28 shows the wire and the contacts naming convention. The results from both methods are presented and discussed.

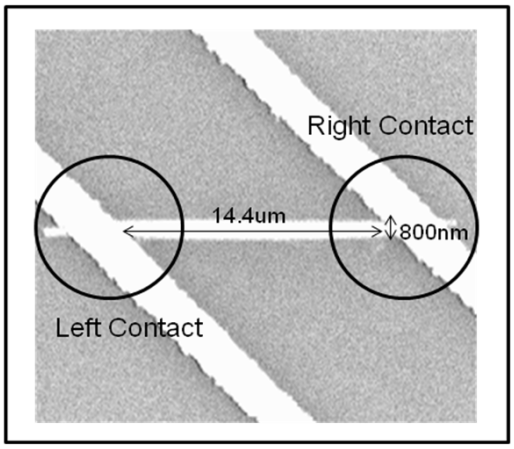

Figure 28. SEM Picture of Sample 1 Taken at 5,000x Magnification

1. Sample 1: Line Scan (Left Contact)

EBIC line scans were performed at both contacts of Sample 1 with the probe current set at $6x10^{-11}$ A and the beam energy at 20 keV. Figure 29 shows the result from line scan done on the left contact. Since the SEM picture gives a representation of the topography of the scanned line, the signal that is generated by the wire can be extracted by superimposing both the EBIC and SEM line profiles. It can be deduced from Figure 29 that the contact-nanowire interface ends at about 2 µm into the scan and the EBIC signal collected after that represents signal from the nanowire only.

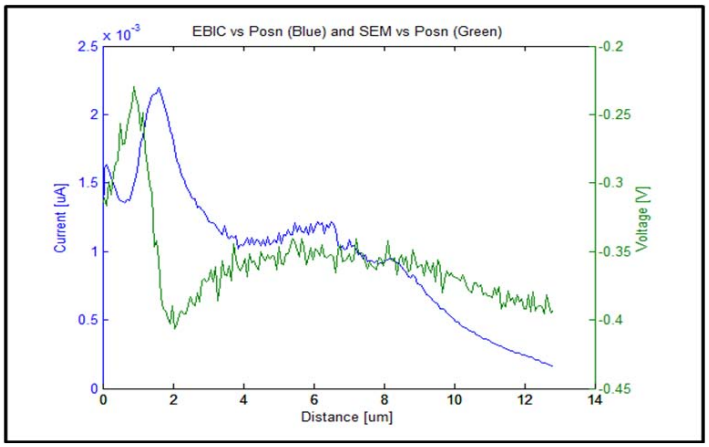

Figure 29. EBIC (Blue) and SEM (Green) Signals as a Function of Position for Sample 1 (Left Contact)

Figure 30(a) shows the portion of the data that is used to extract the diffusion length and Figure 30(b) shows the data fitted to Equation 2.13. The diffusion length is the inverse of the slope of the natural logarithm of the current as a function of distance. The calculated diffusion length, L_d , is 0.62 µm.

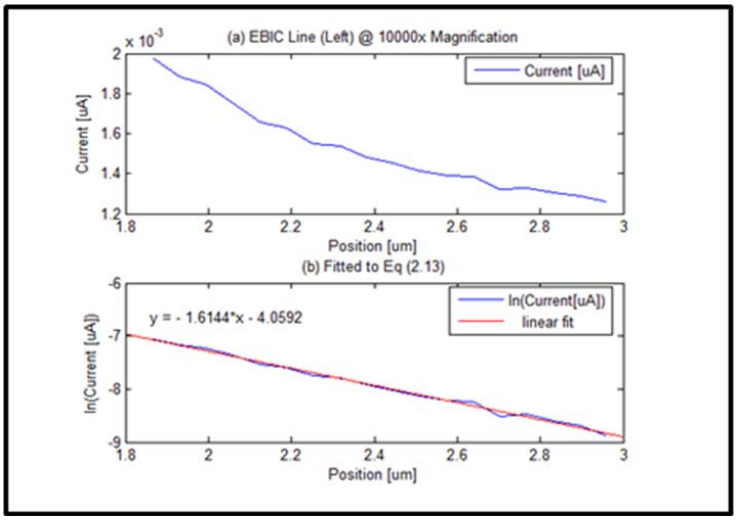

Figure 30. Sample 1 EBIC Line Scan (Left)—(a) Portion of Data Used for Determining Diffusion Length and (b) Data Fitted to Equation 2.13

2. Sample 1: Line Scan (Right Contact)

Figure 31 shows the line scan done on the right contact with probe current set at 6×10^{-11} A and the beam energy at 20 keV. It can be deduced from Figure 31 that the contact-nanowire interface is at about 2 µm before the end of the scan, and the EBIC signal collected before that is due to the wire only.

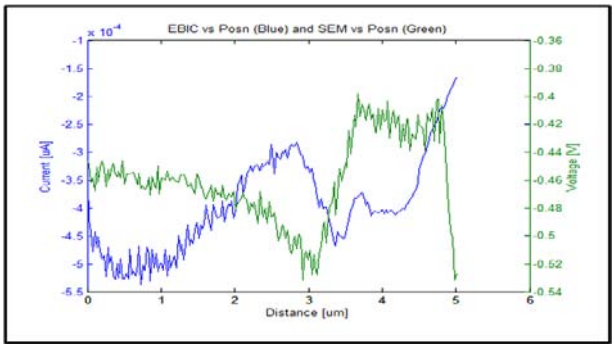

Figure 31. EBIC (Blue) and SEM (Green) Signals as a Function of Position for Sample 1 (Right Contact)

Figure 32(a) shows the portion of the data that is used to extract the diffusion length and Figure 32(b) shows the data fitted to Equation 2.13. The diffusion length is the inverse of the slope of the linear fit line. The calculated diffusion length, L_d , is 0.97 µm. Note that the sign of the slope is arbitrary and it depends on the convention of direction of current flow.

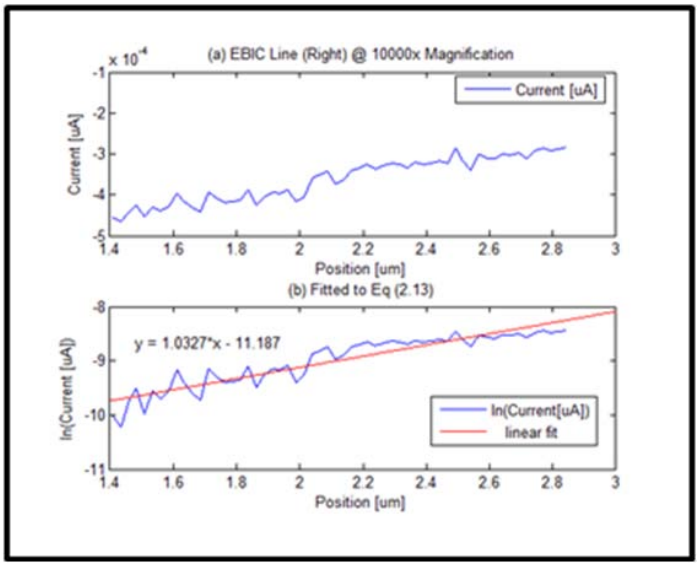

Figure 32. Sample 1: EBIC Line Scan (Right)—(a) Portion of Data Used for Determining Diffusion Length and (b) Data Fitted to Equation 2.13

3. Sample 1: Area Scan (Left)

Area scans were performed on both contacts of Sample 1 with the probe current set at 6×10^{-11} A and the beam energy at 20 keV. Figure 33 shows the EBIC system software readout for an area scan done on the left contact. The color maps depicted by Figure 33(a) and (c) give an overview of the intensities of current and voltage in the scanned area. The current collected is an indication of how the minority charge carrier diffuses in the area whereas the voltage measured is the SEM detector output and an indication of the topography of the scanned area. The same method of superposition can be applied to line profiles of the area scans to get the contact-nanowire boundary and determine the optimum range of data that should be used to calculate diffusion length.

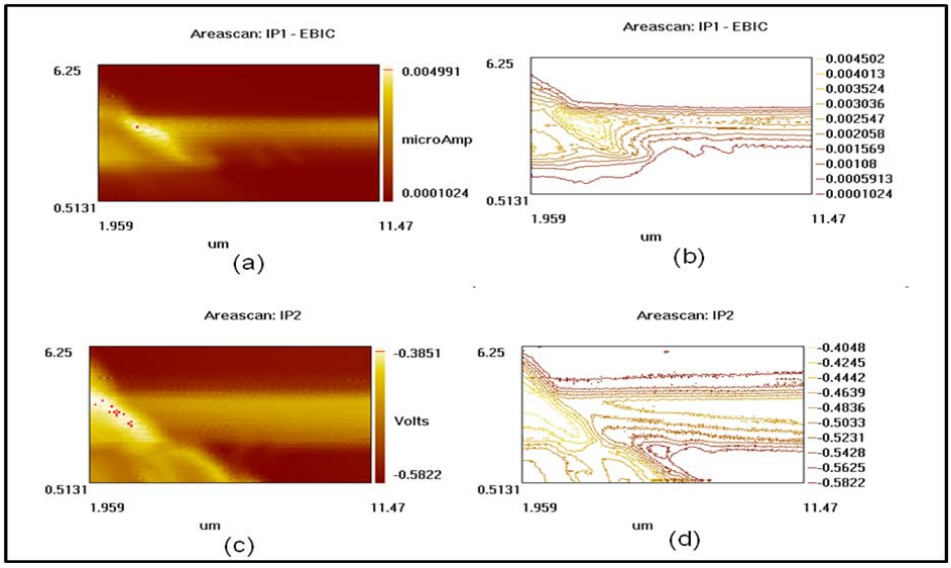

Figure 33. Sample 1 (left contact) EBIC System Software Readout—(a) EBIC Image, (b) EBIC Contour Picture, (c) SEM Image, and (d) SEM Contour Picture

Figure 34 shows the Matlab mesh plots of the same region in three dimensions.

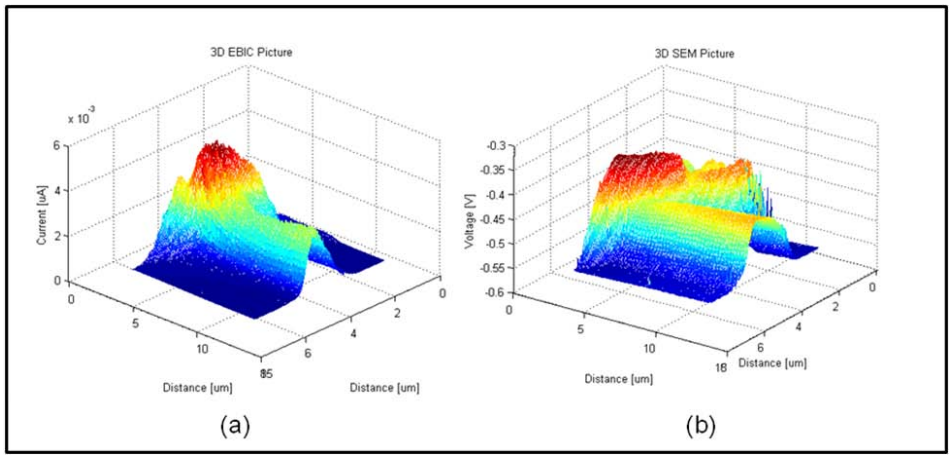

Figure 34. Sample 1 (left) 3-D Plots Using Matlab (a) EBIC and (b) SEM

Figure 35 shows the line profile extracted from the 3-D scans. It can be deduced from Figure 35 that the contact-nanowire interface ends at about 2 µm into the scan, and the EBIC signal collected after that is due to the wire only.

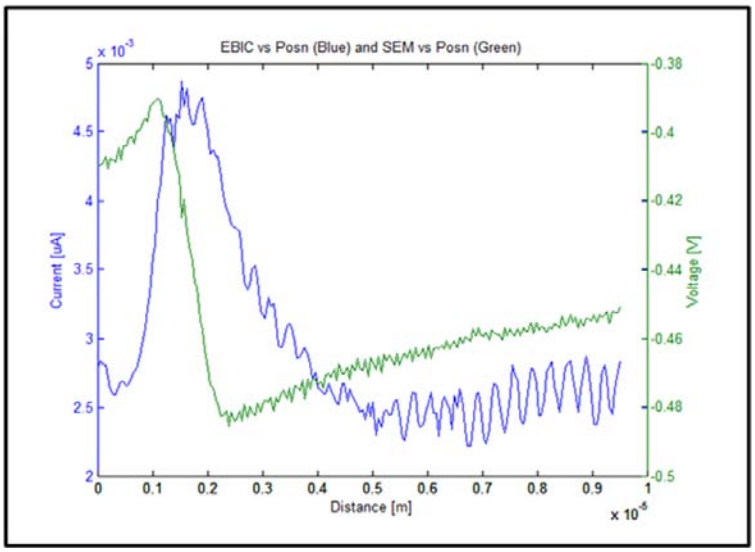

Figure 35. Sample 1 EBIC (Blue) and SEM (Green) Signals as a Function of Distance (Left Contact).

Figure 36(a) shows the portion of the data that is used to extract the diffusion length and Figure 36(b) shows the data fitted to Equation 2.13. The diffusion length is the inverse of the slope of the linear fit line. The calculated diffusion length, L_d , is 0.91 µm.

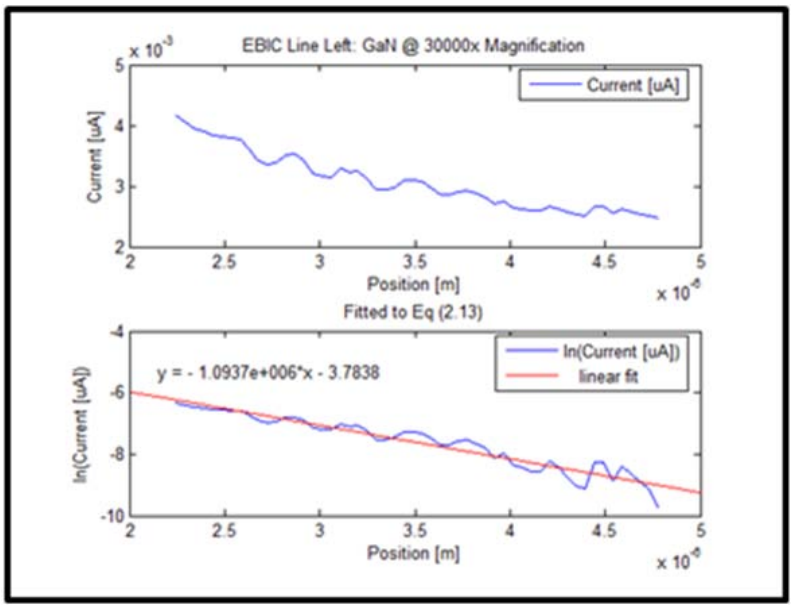

Figure 36. Sample 1 EBIC Line Profile (Left Contact)—(a) Portion of Data Used for Determining Diffusion Length and (b) Data Fitted to Equation 2.13

4. Sample 1: Area Scan (Right)

Figure 37 shows the EBIC system software readout for an area scan done on the right contact with the probe current set at $6x10^{-11}$ A and the beam energy at 20 keV.

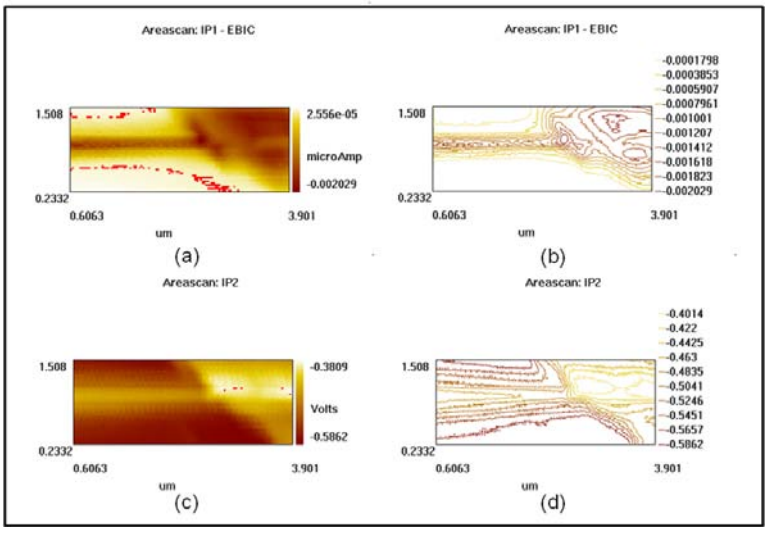

Figure 37. Sample 1 (Right Contact) EBIC System Software Readout—(a) EBIC Image, (b) EBIC Contour Picture, (c) SEM Image, and (d) SEM Contour Picture

Figure 38 shows the Matlab three-dimensional images of the contact and nanowire.

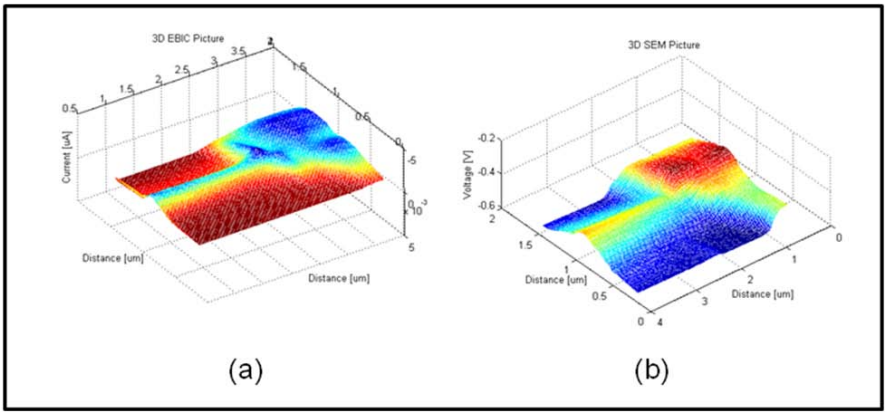

Figure 38. Sample 1 (Right) 3-D Plots Using Matlab (a) EBIC and (b) SEM

Figure 39 shows the line profile extracted from the 3-D scans. It can be deduced from Figure 39 that the contact-nanowire interface ends at about 1.6 µm into the scan and the EBIC signal collected after that is due to the wire only.

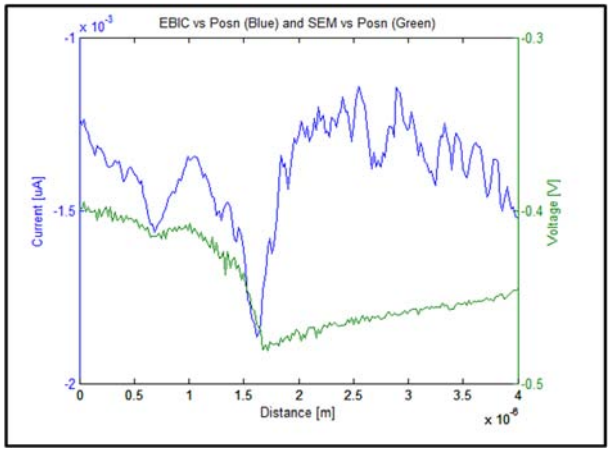

Figure 39. Sample 1 EBIC (Blue) and SEM (Green) Signals as a Function of Distance (Right Contact)

Figure 40(a) shows the portion of the data that is used to extract the diffusion length and Figure 40(b) shows the data fitted to Equation 2.13. The diffusion length is the inverse of the slope of the linear fit line. The calculated diffusion length, L_d, is 1.4 µm.

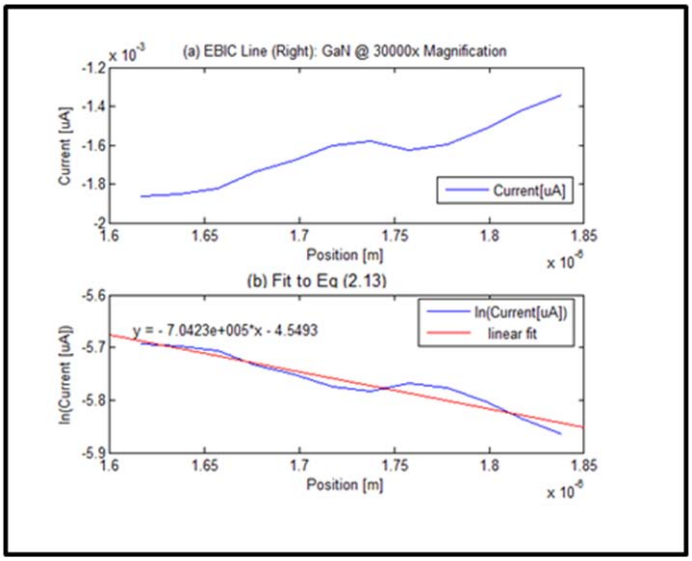

Figure 40. Sample 1 EBIC Line Profile (Right Contact)—(a) Portion of Data Used for Determining Diffusion Length and (b) Data Fitted to Equation 2.13

C. SAMPLE 2: GAN/ALGAN NANOWIRE

Sample is 18.7 µm long and 300 nm wide. Since Sample 2 is not as thick as Sample 1, it is relatively difficult to ensure that the electron beam stayed on the nanowire during line scans. Therefore, diffusion lengths are extracted from the area scans. Similar to Sample 1, the two contacts made are referred to as the left and right contact. Figure 41 shows the wire and the contacts naming convention.

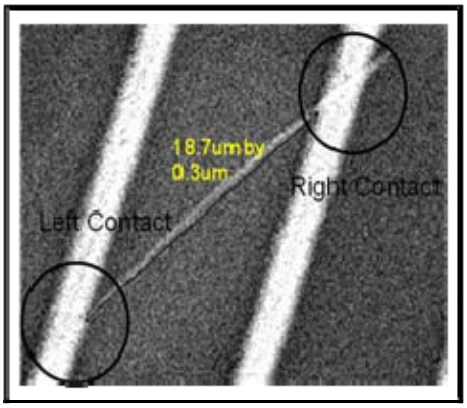

Figure 41. SEM Picture of Sample 2 Taken at 7,000x Magnification

1. Sample 2: Area Scan (Whole)

Area scans are performed on the whole wire to get an overall topography of Sample 2. As shown in Figure 42, the EBIC result of Sample 2 is different from a conventional EBIC map, as highlighted in Figure 22 in Chapter IV. Unlike that of Sample 1, where one contact gives positive EBIC signal and the other gives negative EBIC signal, the EBIC signals on both contacts are negative or positive, depending on which contact is connected to the amplifier and which is connected to the ground). A possible model to explain this observation is presented in Chapter VI.

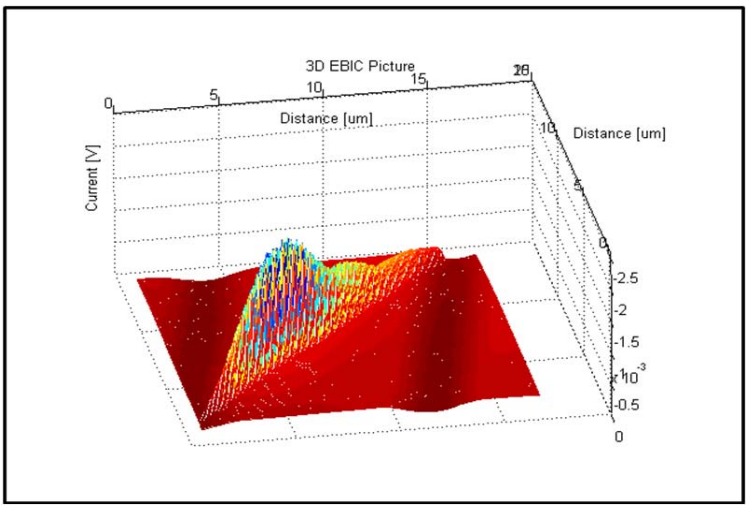

Figure 42. EBIC area Scan of Sample 2 Showing Current Intensity as a Function of Position in *x*- and *y*-axes

2. Sample 2: Area Scan (Left)

Figure 43 shows the EBIC system software readout for an area scan done on the right contact with the probe current set at 6×10^{-11} A and the beam energy at 20 keV.

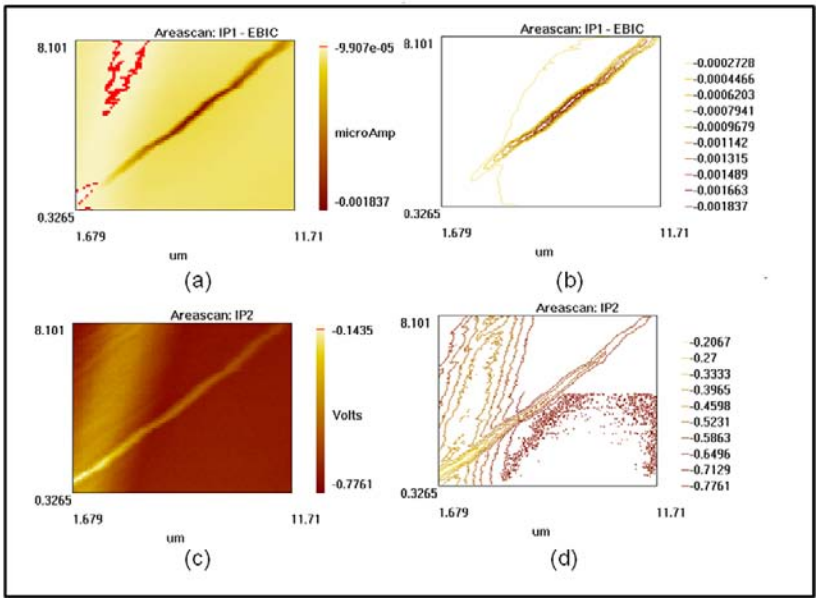

Figure 43. Sample 2 (Left Contact) EBIC System Software Readout—(a) EBIC Image, (b) EBIC Contour Picture, (c) SEM Image, and (d) SEM Contour Picture

Figure 44 shows the Matlab three-dimensional image of the contact and nanowire.

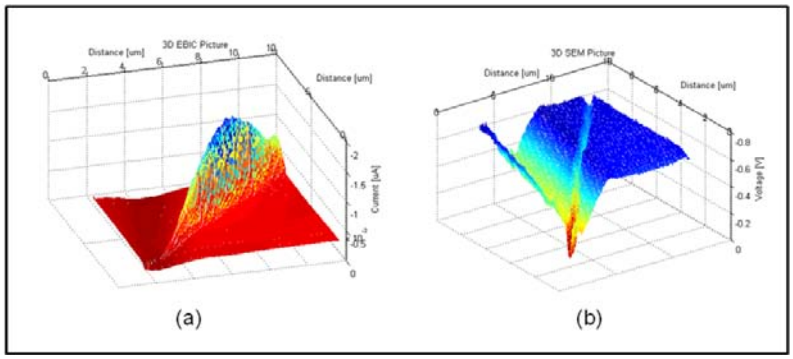

Figure 44. Sample 2 (Left): 3D Plots Using Matlab (a) EBIC and (b) SEM

Figure 45 shows the line profile extracted from the 3D scans. If the contact-nanowire interface is to be extracted from Figure 45, then it is natural to assume that the interface ends about 6 µm into the scan, demarcated by a clear change in the SEM signal. However, if a spatial correlation is made with Figure 44, it is clear that the interface is at about 2 µm into the scan. Therefore, it is taken that the contact-nanowire interface ends at about 2 µm into the scan, and the EBIC signal collected after that is due to the wire only.

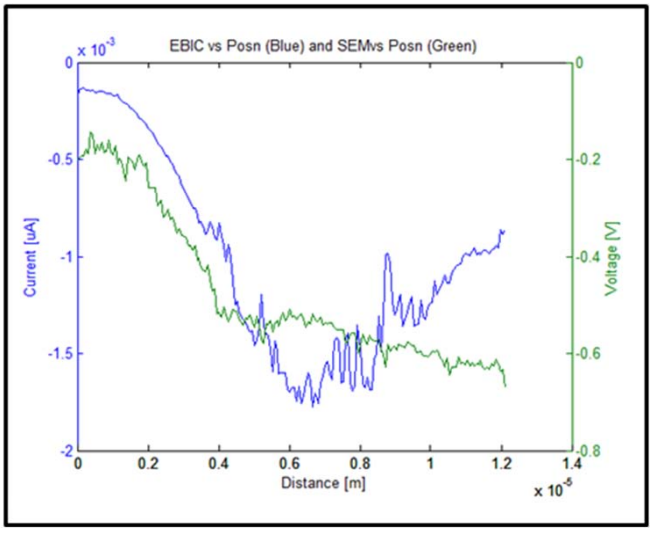

Figure 45. Sample 2 EBIC (Blue) and SEM (Green) Signals as a Function of Position (Left Contact)

Figure 46(a) shows the portion of the data that is used to extract the diffusion length and Figure 46(b) shows the data fitted to Equation 2.13. The diffusion length is the inverse of the slope of the linear fit line. The calculated diffusion length, L_d , is 1.7 µm.

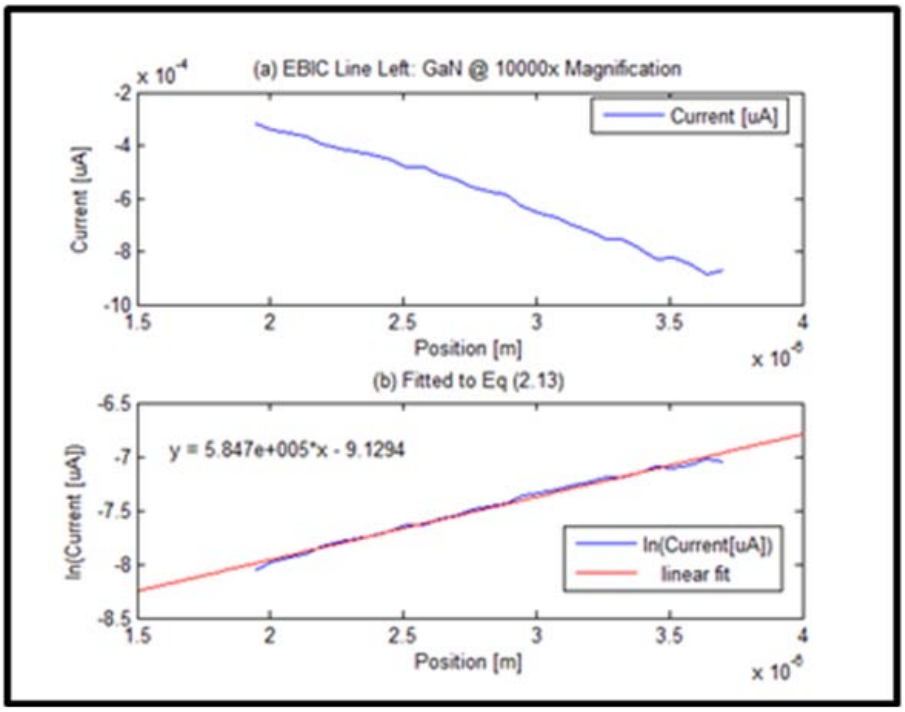

Figure 46. Sample 2 EBIC Line Profile (Left Contact)—(a) Portion of Data used for Determining Diffusion Length and (b) Data Fitted to Equation 2.13

3. Sample 2: Area Scan (Right)

Figure 47 shows the EBIC system software readout for an area scan done on the right contact with the probe current set at 6×10^{-11} A and the beam energy at 20 keV.

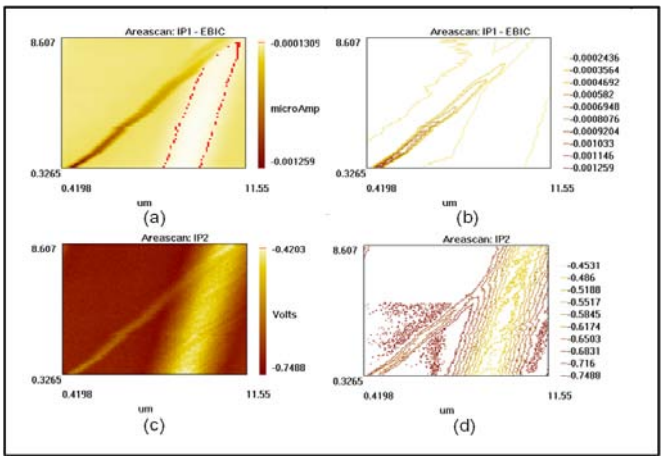

Figure 47. Sample 2 (Right Contact) EBIC System Software Readout—(a) EBIC Image, (b) EBIC Contour Picture, (c) SEM Image, and (d) SEM Contour Picture

Figure 48 shows the Matlab three-dimensional image of the same region on the nanowire.

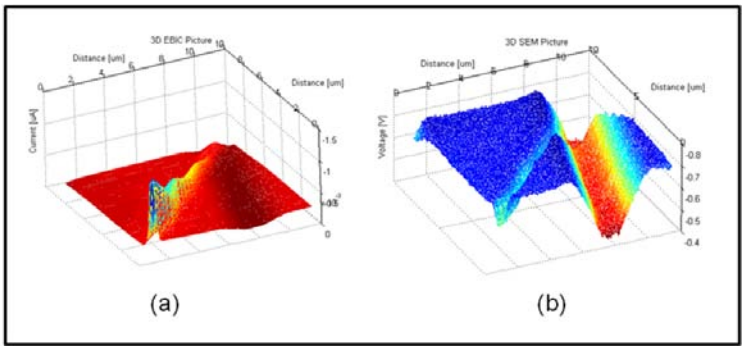

Figure 48. Sample 2 (Right) 3-D Plots Using Matlab (a) EBIC and (b) SEM

Figure 49 shows the line profile extracted from the 3D scans. Similar to the case of Sample 2 (left), the contact-nanowire interface of this experiment has to be extracted by referencing to the Matlab three-dimensional images. As the contact, represented in Figure 48(a) as the small, dark red strip, constitutes only a small portion of the whole scan, it must be deduced from Figure 49 so that the contact-nanowire interface ends at about 12 µm, instead of the 8 µm mark indicated by the clear change in SEM signal, into the scan, and the EBIC signal collected before that is due to the wire only.

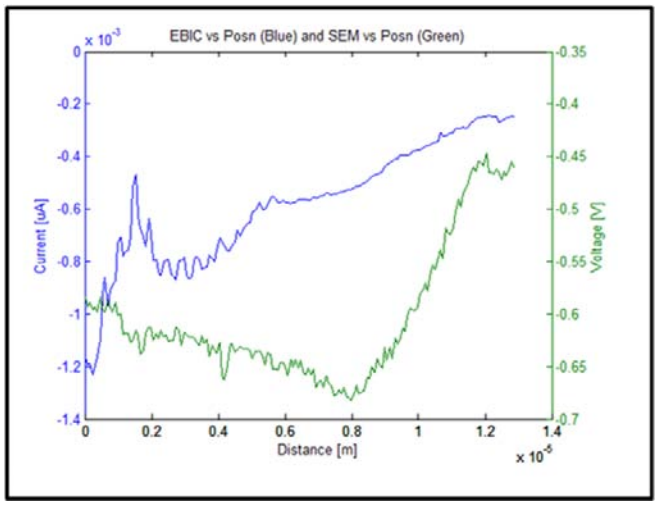

Figure 49. Sample 2 EBIC (Blue) and SEM (Green) Signals as a Function of Position (Right Contact)

Figure 50(a) shows the portion of the data that is used to extract the diffusion length and Figure 50(b) shows the data fitted to Equation 2.13. The diffusion length is the inverse of the slope of the linear fit line. The calculated diffusion length, L_d, is 2.4 µm. A possible explanation for the relatively long diffusion length is discussed in Chapter VI.

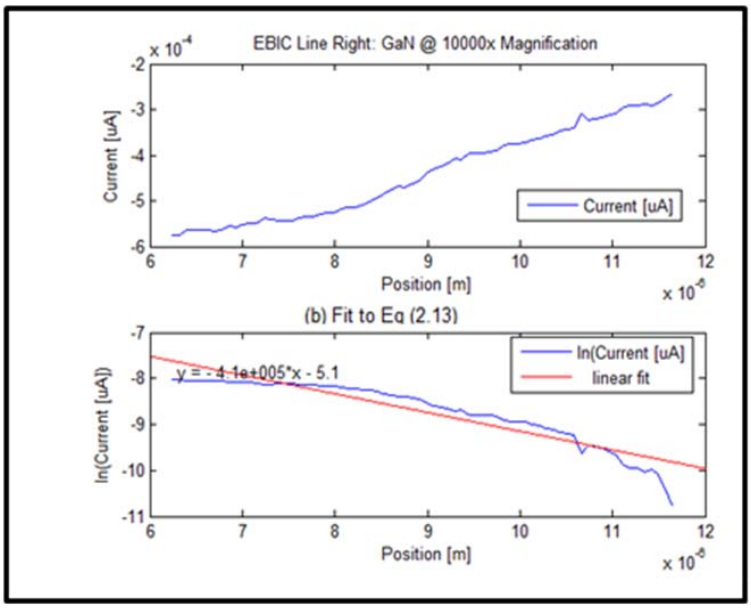

Figure 50. Sample 2 EBIC Line Profile (Right Contact)—(a) Portion of Data Used for Determining Diffusion Length and (b) Data Fitted to Equation 2.13

D. SAMPLE 3: UNCOATED GAN NANOWIRE

Sample 3 contains two uncoated UID GaN nanowires. Sample 3a is 1.5 µm long and 230 nm thick and Sample 3b is 6 µm long and 170 nm thick. Similar to Sample 2, it is very difficult to ensure that the electron beam does not drift off these thin nanowires during line scans. Therefore, the diffusion length must be extracted from area scans. Figure 51 shows the SEM picture of samples 3a and 3b and their dimensions.

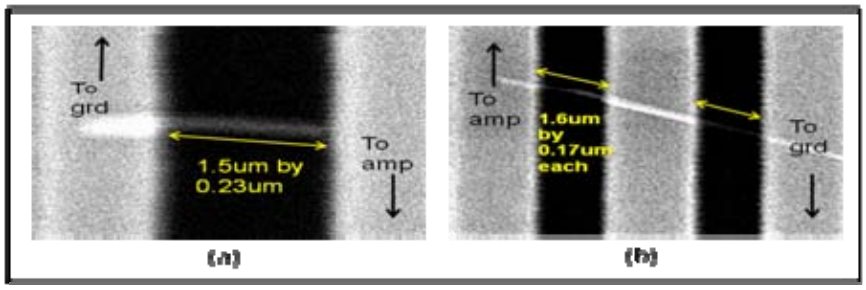

Figure 51. SEM Picture of (a) Sample 3a Taken at 30,000x Magnification and (b) Sample 3b Taken at 10,000x Magnification.

1. Sample 3a: Area Scan

Figure 52 shows the EBIC system software readout for an area scan done on Sample 3a with the probe current set at $6x10^{-11}$ A and the beam energy at 20 keV.

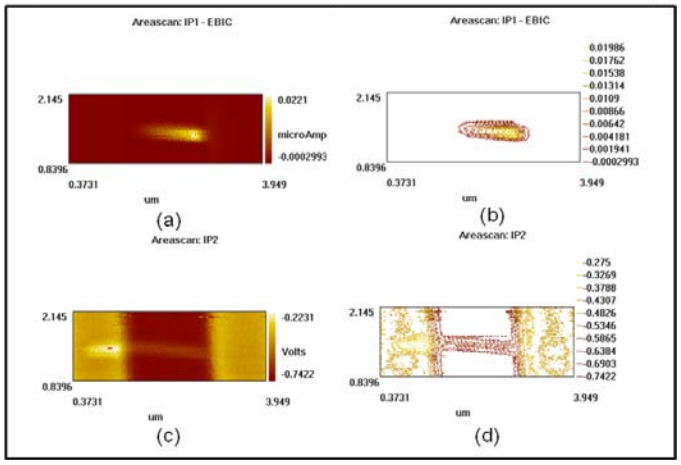

Figure 52. Sample 3a EBIC System Software Readout—(a) EBIC image, (b) EBIC Contour Picture, (c) SEM Image, and (d) SEM Contour Picture

Figure 53 shows the Matlab three-dimensional image of the contact and nanowire.

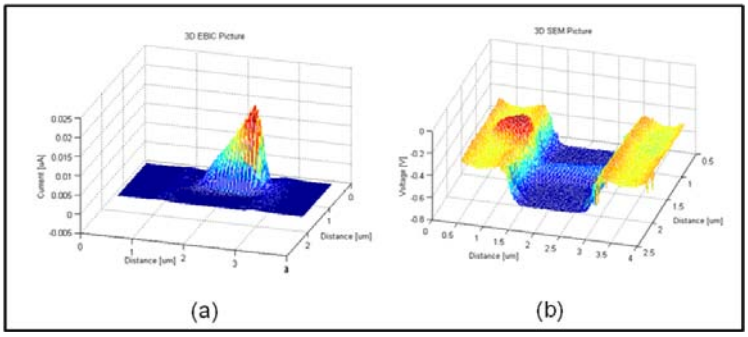

Figure 53. Sample 3a 3-D Plots Using Matlab (a) EBIC and (b) SEM

Figure 54 shows the line profile extracted from the 3-D scans. It can be deduced from Figure 54 that the contact-nanowire interface ends at about 1 µm into the scan and the EBIC signal collected after that is due to the wire only. It can be observed that the EBIC signal is slightly different from that of Samples 1 and 2, in that only 1 decay slope is observed (from 1 µm to about 2.5 µm). This is due to the small inter-contact distance, resulting in minority charge carriers being collected throughout the entire region. However, diffusion length can still be extracted from the slope of the decay. This phenomenon is true for all the nanowires in Sample 3.

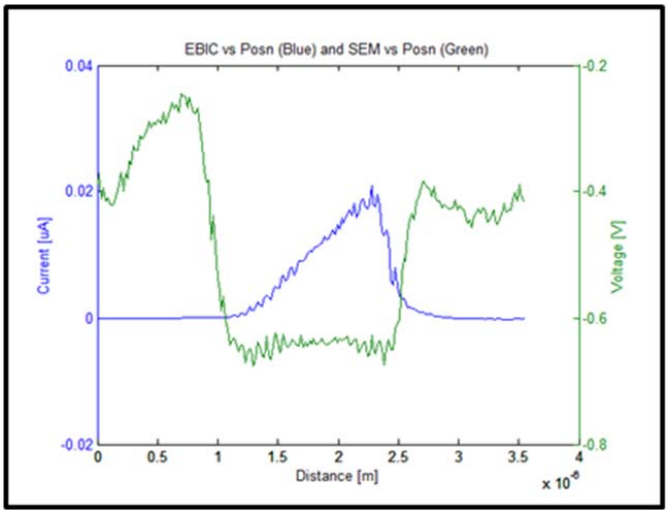

Figure 54. Sample 3a EBIC (Blue) and SEM (Green) Signals as a Function of Position

Figure 55(a) shows the portion of the data that is used to extract the diffusion length and Figure 55(b) shows the data fitted to Equation 2.13. The diffusion length is the inverse of the slope of the linear fit line. The calculated diffusion length, L_d , is 0.40 µm.

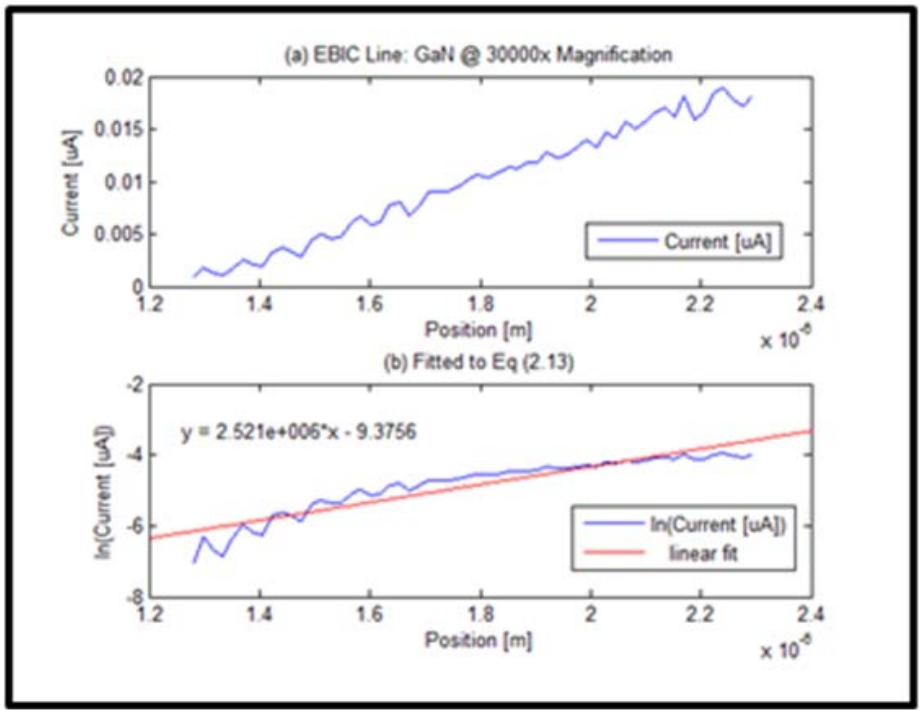

Figure 55. Sample 3a EBIC Line Profile—(a) Portion of Data Used for Determining Diffusion Length and (b) Data Fitted to Equation 2.13

2. Sample 3b: Area Scan

Figure 56 shows the EBIC system software readout for an area scan done on Sample 3b with the probe current set at 6×10^{-11} A and the beam energy at 20 keV. Since Sample 3b is contacted via three contact probes, the first experiment aims to measure the EBIC spanning the whole wire.

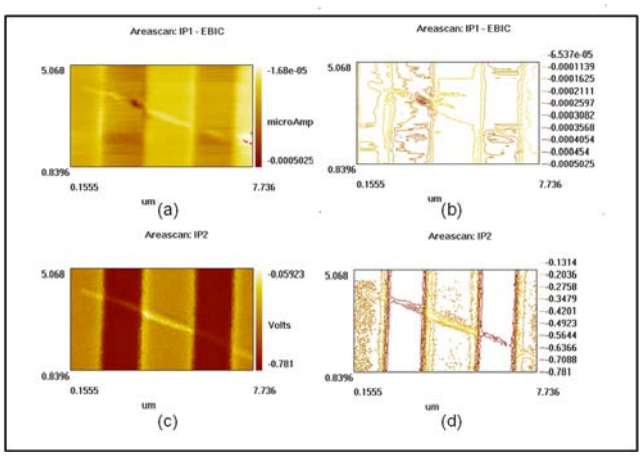

Figure 56. Sample 3b EBIC System Software Readout—(a) EBIC image, (b) EBIC Contour Picture, (c) SEM Image, and (d) SEM Contour Picture

Figure 57 shows the Matlab three-dimensional image of the contact and nanowire. The blue colour spike seen in Figure 58(a) corresponds with the dark red spot in Figure 56(a).

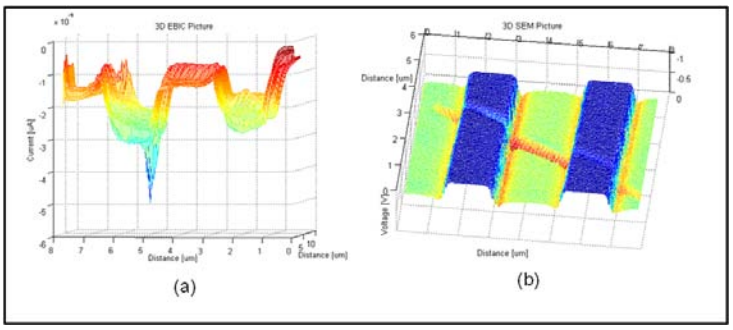

Figure 57. Sample 3b 3-D Plots Using Matlab (a) EBIC and (b) SEM

Figure 58 shows the line profile extracted from the 3-D scans. It can be deduced from Figure 58 that the blue spike in Figure 57(a) is the corresponding peak between 2 µm and 3 µm. While there may seem to be another secondary red peak in Figure 57(a), it is the strong EBIC signal generated by the wire directly under the metal contact. This becomes apparent when a matching is done on the line profile between the EBIC and SEM picture. See Figure 58, depicted by the overlap between 0.6 µm to 1.8 µm. Similar to Sample 3a, only one area scan is done on this sample.

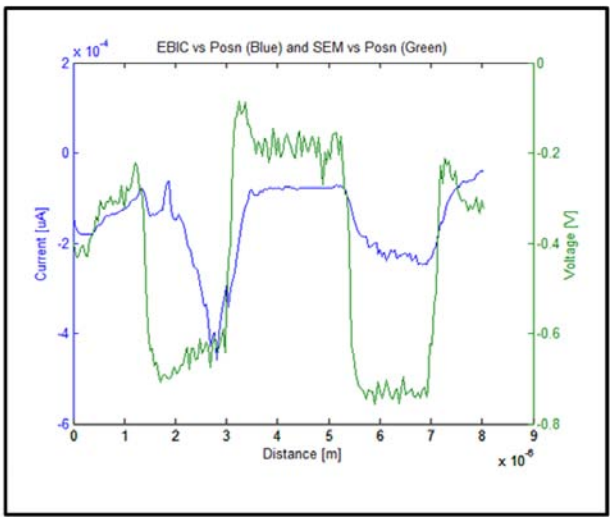

Figure 58. Sample 3b EBIC (Blue) and SEM (Green) Signals as a Function of Position

Figure 59(a) shows the portion of the data that is used to extract the diffusion length and Figure 59(b) shows the data fitted to Equation 2.13. The diffusion length is the inverse of the slope of the linear fit line. The calculated diffusion length, L_d, is 0.55 µm.

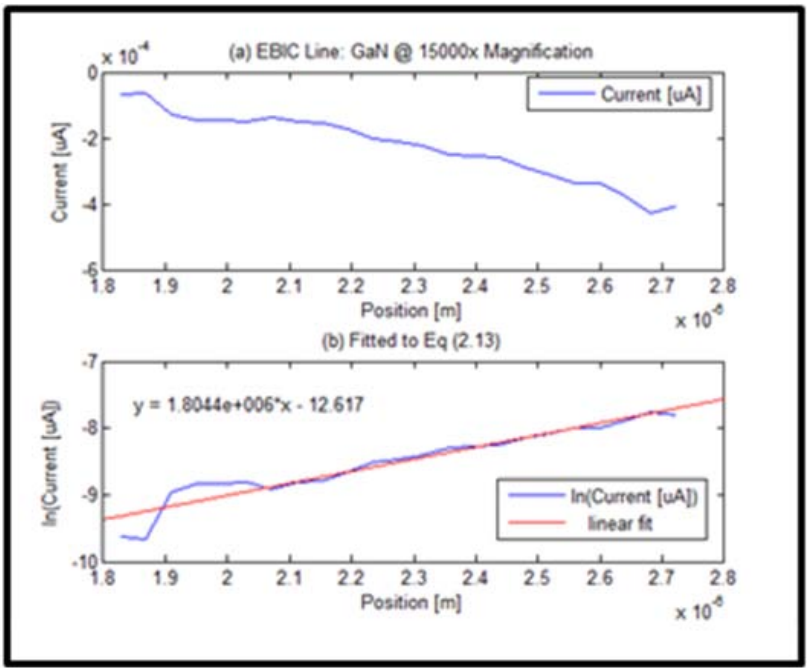

Figure 59. Sample 3b EBIC Line Profile—(a) Portion of Data Used for Determining Diffusion Length and (b) Data Fitted to Equation 2.13

3. Sample 3b: Area Scan (Configuration 1)

Since Sample 3b is contacted via three metal probes, two more experiments are conducted using the configurations shown in Figure 60. By contacting the metal probes using the configurations in Figure 60, Sample 3b is effectively “broken” into two smaller nanowires.

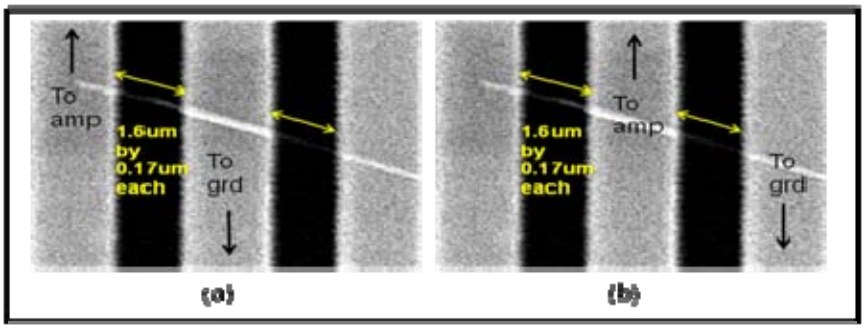

Figure 60. “Breaking” Sample 3b into Two Shorter Wires—(a) Configuration 1 and (b) Configuration 2

Figure 61 shows the EBIC system software readout for an area scan done on Configuration 1 with the probe current set at 6×10^{-11} A and the beam energy at 20 keV.

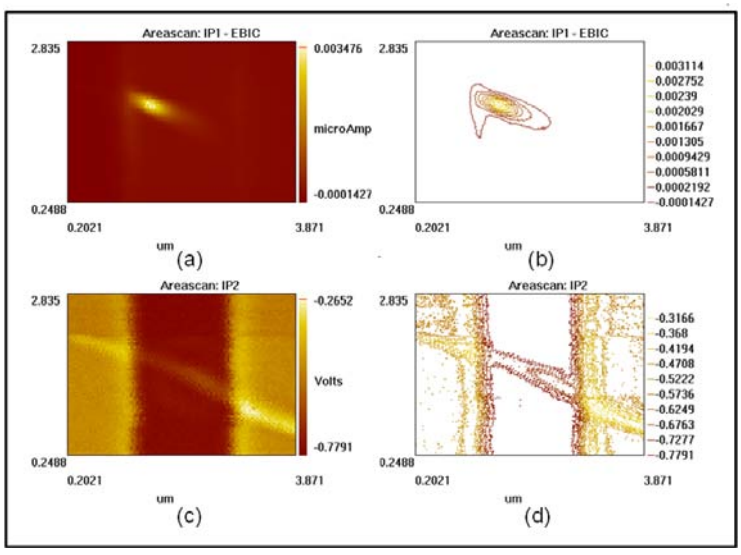

Figure 61. Sample 3b (Configuration 1) EBIC System Software Readout—(a) EBIC Image, (b) EBIC Contour Picture, (c) SEM Image, and (d) SEM Contour Picture

Figure 62 shows the Matlab three-dimensional image of the contact and nanowire.

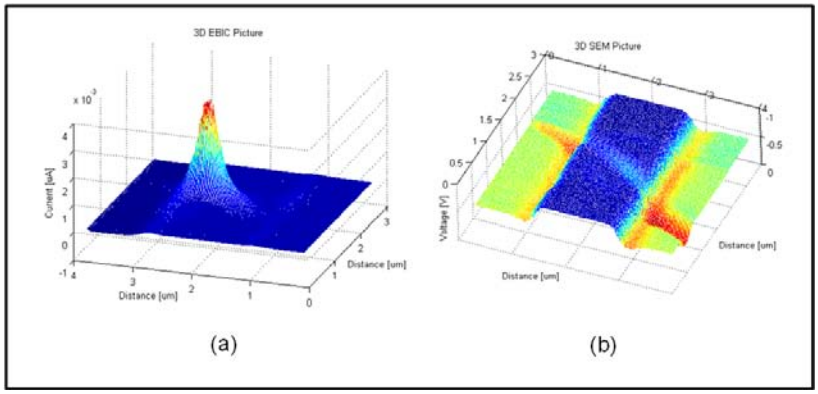

Figure 62. Sample 3b (Configuration 1) 3-D Plots Using Matlab (a) EBIC and (b) SEM

Figure 63 shows the line profile extracted from the 3-D scans. It can be deduced from Figure 63 that the metal-nanowire interface ends at about 1.3 µm into the scan. Similar to Sample 3a, the close proximity of the metal contacts does not allow for independent left and right contact scans.

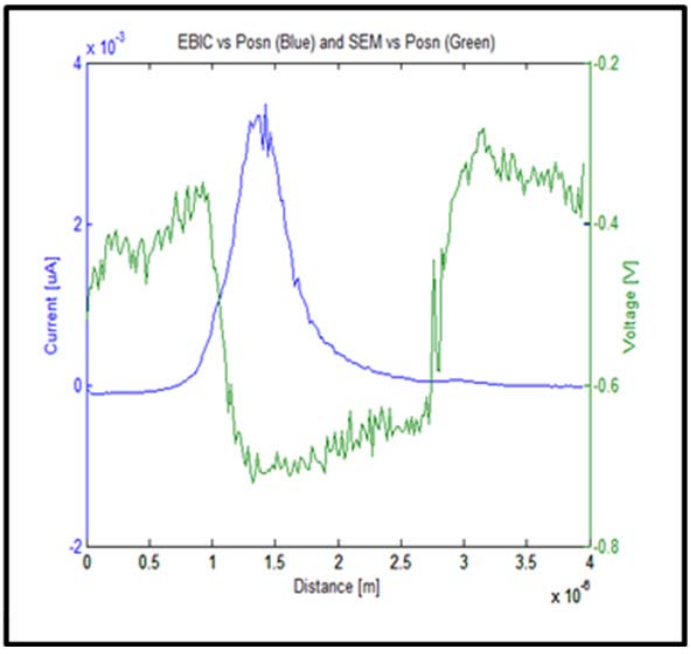

Figure 63. Sample 3b (Configuration 1) EBIC (Blue) and SEM (Green) Signals as a Function of Position

Figure 64(a) shows the portion of the data that is used to extract the diffusion length and Figure 64(b) shows the data fitted to Equation 2.13. The diffusion length is the inverse of the slope of the linear fit line. The calculated diffusion length, L_d , is 0.26 µm.

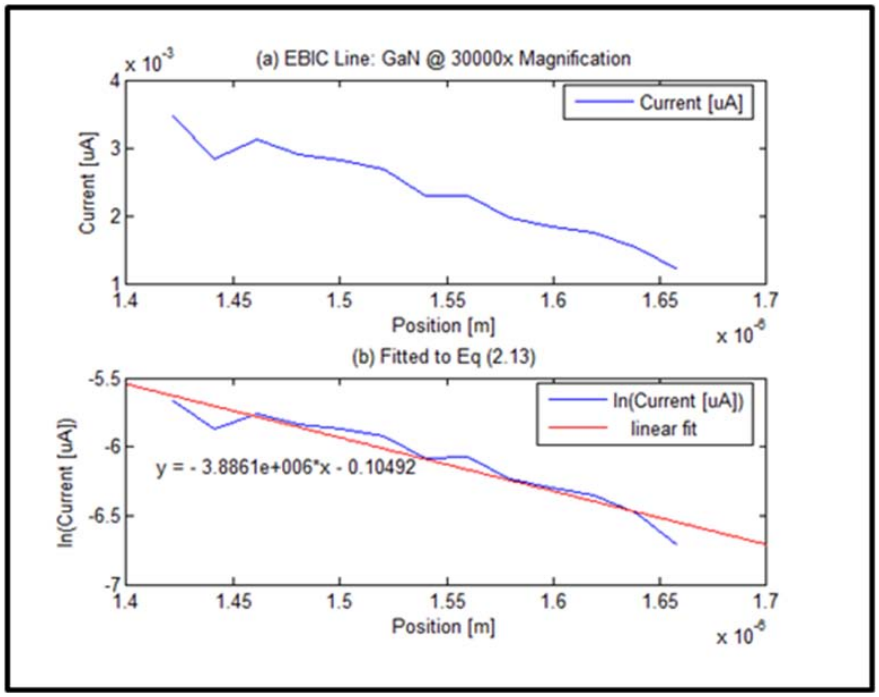

Figure 64. Sample 3b (Configuration 1) EBIC Line Profile—(a) Portion of Data Used for Determining Diffusion Length and (b) Data Fitted to Equation 2.13

4. Sample 3b: Area Scan (Configuration 2)

Figure 65 shows the EBIC system software readout for an area scan done on Configuration 2 with the probe current set at 6×10^{-11} A and the beam energy at 20 keV. Unfortunately, the signal generated under this configuration is too small to justify any further analysis. This is consistent with the readout from Figure 57 and Figure 60 whereby any signal collected in this part of the wire is either very weak or embedded within the noise.

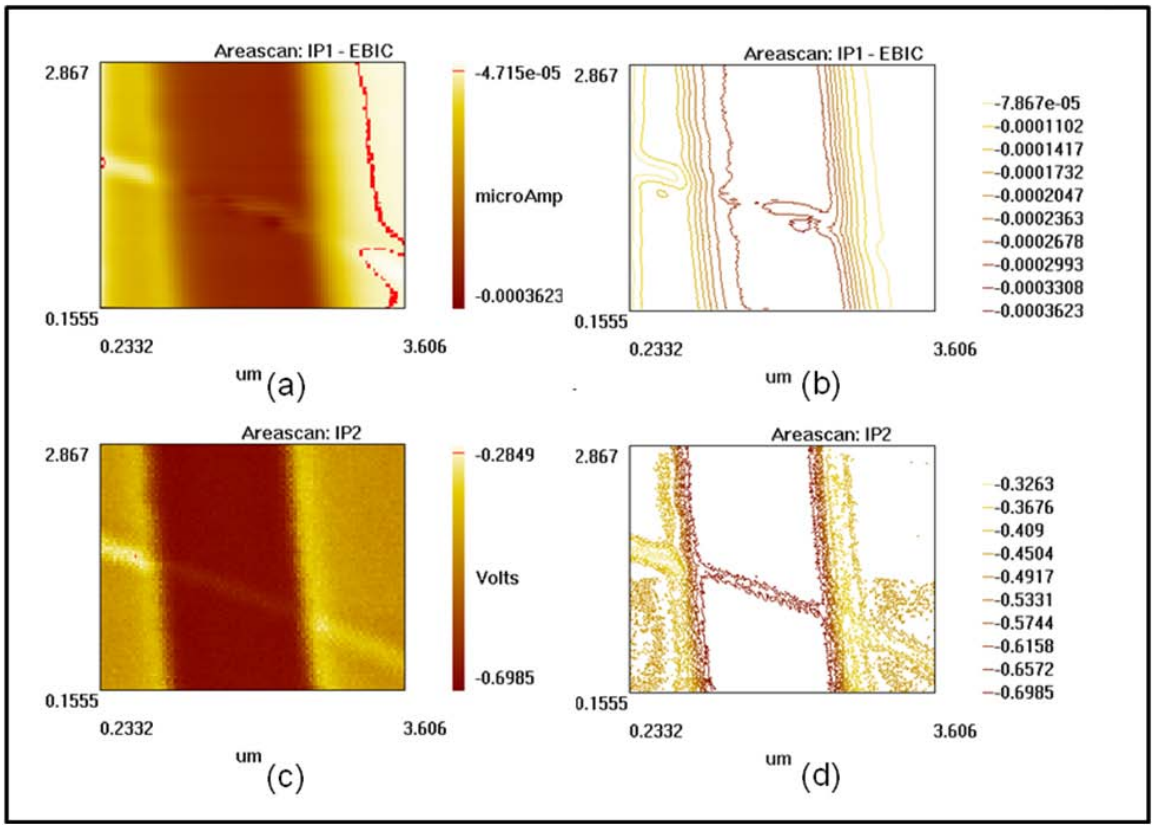

Figure 65. Sample 3b (Configuration 2) EBIC System Software Readout—(a) EBIC Image, (b) EBIC Contour Picture, (c) SEM image, and (d) SEM Contour Picture

THIS PAGE INTENTIONALLY LEFT BLANK

VI. CONCLUSIONS AND SUGGESTIONS FOR FURTHER RESEARCH

A. SUMMARY OF RESULTS

The results of Sample 1 note that the difference in diffusion length measured by just conducting a line scan is about 46 percent lower than that obtained from the area scan. This trend is consistent with the effect of the beam moving off the wire due to vibrational effects. In order to make the comparison more consistent, the diffusion length of the nanowire is that which is obtained from area scan. As such, the diffusion length of Sample 1 (AlGaN coated GaN nanowire) is found to be 1.2 μm, with a standard deviation of 22 percent, based on two area measurements assuming that the left and right sides are identical. The diffusion length of Sample 2 (AlGaN coated GaN nanowire) is found to be 2.1 μm, with a standard deviation of 18 percent. In addition, the diffusion length of Sample 3 (uncoated GaN nanowire) is found to be 0.40 μm, with a standard deviation of 24 percent. The results are summarized in Tables 3 through 5.

Table 3. Summary of Diffusion Length Data for Sample 1

Sample 1				
Diffusion length, L_d	Left	Right	$\overline{L_d} \pm \sigma$	$\overline{L_d} \pm \sigma(\%)$
Line	0.62 μm	0.97 μm	0.80 ± 0.18 μm	0.80 μm ± 22%
Area	0.91 μm	1.4 μm	1.2 ± 0.26 μm	1.2 μm ± 22%
$\overline{L_d} \pm \sigma$	0.77 ± 0.15 μm	1.2 ± 0.23 μm	0.98 ± 0.22 μm	--
$\overline{L_d} \pm \sigma(\%)$	0.77 μm ± 19%	1.2 μm ± 19%	--	0.98 μm ± 22%

Table 4. Summary of Diffusion Length Data for Sample 2

Sample 2				
Diffusion length, L_d	Left	Right	$\overline{L_d} \pm \sigma$	$\overline{L_d} \pm \sigma(\%)$
Area	1.7 μm	2.4 μm	2.1 ± 0.37 μm	2.1 μm ± 18%

Table 5. Summary of Diffusion Length Data for Sample 3

Sample 3					
Diffusion length, L_d	Sample 3a	Sample 3b	Sample 3b (Config 1)	$\overline{L_d} \pm \sigma$	$\overline{L_d} \pm \sigma(\%)$
Area	0.40	0.55	0.26	0.40 ± 0.098 μm	0.40 μm ± 24%

While it is assumed that the left and right contacts are the same, it is possible that they can be different given that the electrical properties of the wire are strongly dependent on the growth conditions. One possible difference is the level of doping. Since mobility is dependent on the doping concentration and it is difficult to ensure uniform doping when growing the nanowire, the dopant concentration in both ends of the wire could very well be different. Also, since the geometry of nanowire is such that the aspect ratio of radius to length is large compared to bulk materials, it is believed that there is a strong dependence between current and the diameter and total surface area of the nanowire. This is consistent with the observation in Samples 1 and 2 that the diameter of the wire near the right contact is slightly bigger than that near the left contact (see Figures 28 and 41), and so the diffusion length calculated is also larger than that of the left contact. The results in this thesis are consistent with the hypothesis presented in [30], that drift current is proportional to the cross sectional area of the wire and is also scaled by the aspect ratio.

The diffusion length in the uncoated wires is also expected to be smaller than that in the coated wires. The AlGaN coating, having a larger energy gap, acts as a barrier confining the minority charge carriers within the core GaN wire.

Therefore, losses due to surface recombination are smaller than that of the uncoated wires and thus resulting in a longer minority charge carrier diffusion length.

In an independent and parallel study of minority charge carrier diffusion lengths in similar coated and uncoated GaN nanowires using NSOM done by LCDR Lee Baird, the diffusion length obtained is summarized in Table 6 [31].

Table 6. Diffusion Lengths Measured Using NSOM (After [31])

Sample	Diffusion length, L_d
GaN/AlGaN nanowires	1.3 ± 0.20 μm
GaN uncoated nanowires	0.96 ± 0.25 μm

B. ISSUES FOR FURTHER ANALYSIS

1. Asymmetry in EBIC Signals

It was observed in the course of this thesis work that there is an unexpected asymmetry in the EBIC signals that are being collected for the case of the uncoated wires with short inter-contact spacing. Since the two contacts are initially identical and there is no applied external bias, the EBIC signals should behave the same way independent of which contact is connected to the amplifier. Figure 66 shows the expected symmetry of the EBIC signals when the contact connected to the amplifier is switched. In both cases, a positive current should be recorded adjacent to the contact that is connected to the amplifier.

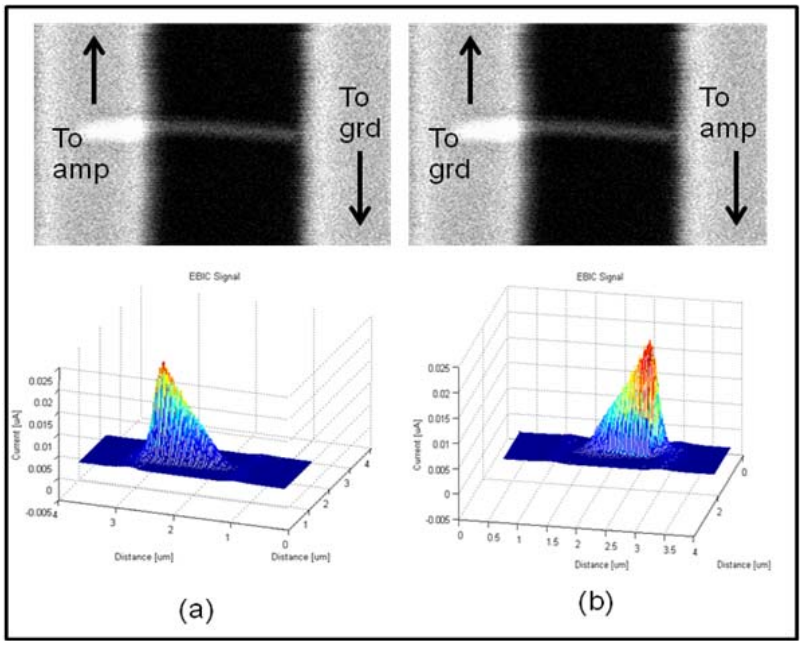

Figure 66. Expected Symmetric EBIC Signals

The observed EBIC signals behaved differently in response to changes in the amplifier configuration. Figure 67 shows the observed EBIC signals when the contact connected to the amplifier is switched. Instead of being symmetrical about the vertical axis, the observed result is symmetrical about the horizontal axis and a negative current was measured instead.

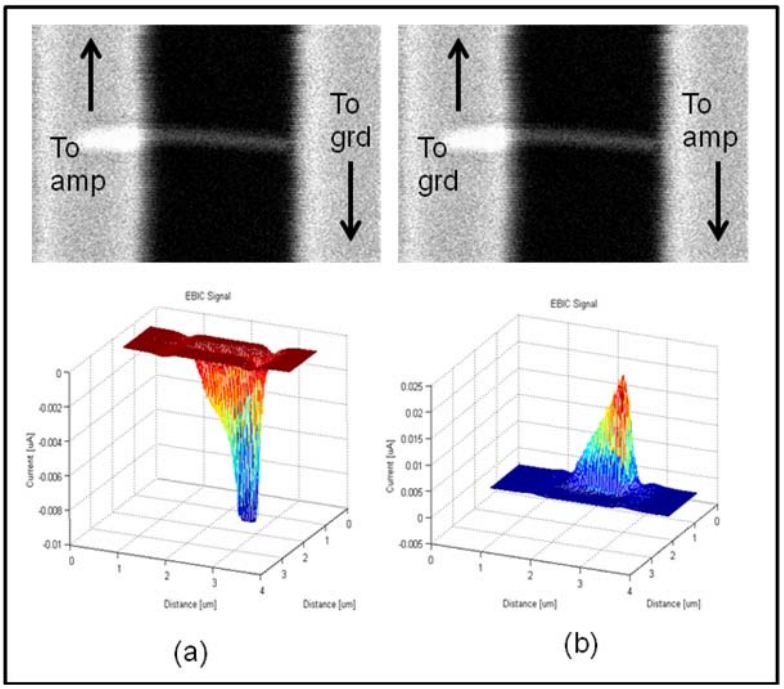

Figure 67. Observed Asymmetric EBIC Signals

Since all other parameters remain constant during the two experiments (i.e., probe current and energy of electron beam), this behavior seem to suggest that there is a preferred flow direction for the minority charge carriers. A possible explanation for this behavior is that there exists a region on the surface of the nanowire where space-charges were built up because of electron beam excitation. This trapping of charge has, in turn, created an E-field that preferences the direction of flow of the minority charge carriers.

A similar explanation was proposed in [19] where carrier concentration and mobility in GaN nanowires were measured under UV illumination. It was found that the currents in wires with small diameters—a range of 200 to 300 nm—decreases by as much as 20 percent between the time when the wire is exposed to UV illumination and after 15 hours in the dark. The researchers proposed that the difference is due to the difference in the size of the conducting channel. When the wire is illuminated, charges are trapped in the gate-oxide layer, thus, reducing the size of the conducting channel. When the sample is allowed to relax in the dark for up to 15 hours, the trapped charges dissipate and

higher currents are measured because of a larger conduction channel. Using a similar argument, it is possible that charge trapping happens the moment the nanowire is excited by the SEM electron beam. These trapped charges then create an E-field that preferences the direction of flow of minority charge carriers.

2. EBIC Result for Sample 2

The EBIC signal from Sample 2 is different from the other nanowire samples. As opposed to decreasing diffusive current being collected as the electron beam moves farther away from the contact, the signal from Sample 2 is characterized as having more diffusive current as the electron beam moves away from the contacts. See Figure 35 and Figure 43 in Chapter V. When the sample was re-examined under a higher resolution SEM after the EBIC experiments, it was found that the AlGaN coating was removed from the core GaN nanowire near the center of the wire. Figure 68 shows a picture of “post EBIC” Sample 2 with a magnified insert of the portion of the wire where the AlGaN coating was disturbed. While it is suspected that the repeated localized heating and cooling due to the numerous EBIC experiments conducted on Sample 2 might have caused the AlGaN coating to peel off, the exact cause of higher diffusive current is recorded away from the contact is still unknown. It is possible that the uncoated region creates an effective junction in the center of the device that dominates the field effects at the contacts. Additional experiments would have to be conducted on nanowires of similar length, diameter and inter-contact distance in order to confirm this hypothesis.

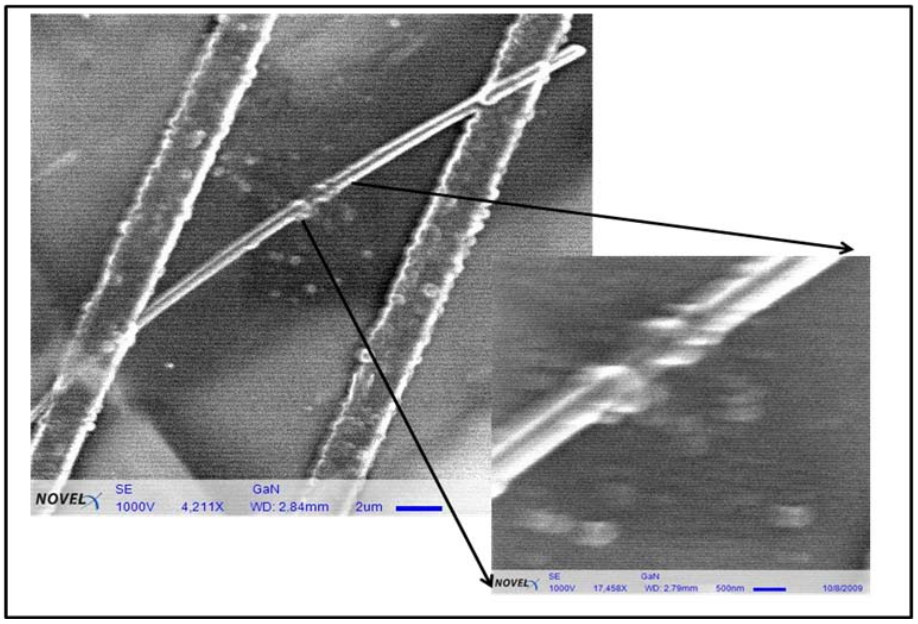

Figure 68. High Resolution SEM Picture of "Post-EBIC" Sample 2 Taken at 4,000x and 17,000x Magnification

C. SUGGESTIONS FOR FUTURE RESEARCH

1. Map Diffusion Length as a Function of Diameter of Nanowire

Due to limited time and availability of samples, it is not possible to have a database of diffusion length as a function of the diameter of the nanowire. Such a comparison will be beneficial in understanding the validity and limits of the assumption that charge carriers in nanowires are confined to one axis of movement. Furthermore, if the database is large enough, conclusions can be made to determine the crossover between confining charge carriers to one or two axes of movement.

2. Simulate the Space-Charge Effect

As mentioned in the previous section, the effects of space-charge built up by the double Schottky barrier are important and have not been understood fully. It would be beneficial for further understanding of nano structures if the space-charge phenomenon can be simulated and tested so that its effects can be accounted for.

3. Create Schottky-Ohmic Contact Pair

As mentioned in the earlier section, a possible cause of the asymmetry of the EBIC signal is the existence of two Schottky barriers. In traditional EBIC experiments, it is always assumed that there exists a Schottky-Ohmic contact pair and the signal measured is purely due to the collection at a single Schottky barrier. As highlighted in Chapter III, the ratio between the inter-contact distance and the length of nanowire cannot be assumed to be small and therefore ignored. It is important that a Schottky-Ohmic contact pair be made so that the number of uncontrollable variables can be kept to a minimum. With such a contact pair, the effects of any space-charge phenomenon can possibly be isolated and eliminated and the measured EBIC may be more accurate as it is closer to a traditional EBIC setup.

D. CONCLUSION

This thesis has achieved its primary aim to independently measure the minority charge carrier diffusion length in GaN nanowires using EBIC. The results indicate larger L_d in GaN/AlGaN wires due to the barrier effect of the AlGaN layer. The results for the GaN/AlGaN (core-shell) nanowires are comparable to that obtained via the independent NSOM method and the results for the uncoated GaN nanowires are within 58 percent. This satisfies the secondary aim of this thesis to validate the accuracy and feasibility of using NSOM and transport imaging methods to measure diffusion length.

During the course of this work, little published literature was found on the diffusion length of minority charge carriers in GaN nanowires. As such, this thesis can be considered a pioneering attempt in measuring and understanding the works of minority charge carriers in GaN nanowires. Not only is the diffusion length measured, this thesis has also established and documented a systematic way to conduct the experiment to measure minority charge carrier diffusion length in GaN nanowire. This work can serve as a reference for future studies in the similar fields.

This thesis has also drawn possible links to the existence of surface-related space-charge behavior in nanostructures as presented in the works of L.M.Mansfield's group from NIST [19] and aspect ratio dependence in A.A.Talin's group in Sandia National Laboratories [30]. It is clear that surface charge effects, and their transient behavior, will play a key role in understanding the electronic properties of these structures. In order to improve the quality of using EBIC as a possible technique to measure minority charge carrier diffusion length in nanowires, more work needs to be done to create a good Schottky-Ohmic contact pair.

THIS PAGE INTENTIONALLY LEFT BLANK

LIST OF REFERENCES

[1] N.Taniguchi, *On the Basic Concept of Nano-technology*, Proc Intl Conf Prod London, Part II British Society of Precision Engineering, 1974.

[2] Wikipedia, Nanotechnology, http://en.wikipedia.org/wiki/Nanotechnology (Last accessed 11 Nov 2009).

[3] N.M.Haegel, J.D.Fabbi and M.P.Coleman, *Direct transport imaging in planar structures*, Applied Physics Letters, 84, 1329, 2004.

[4] D.R.Luber, F.M.Bradley, N.M.Haegel, M.C.Talmadge, M.P.Coleman, T.D.Boone, *Imaging transport for the determination of minority carrier diffusion length*, Applied Physics Letters, 88, 163509, 2006.

[5] C.H.Low, *Near field scanning optical microscopy (NSOM) of nano devices*, Master's Thesis, Naval Postgraduate School, 2008.

[6] D.Kharat, H.Muthrajan, B.Praveenkumar, *Present and future military applications of nanodevices*, Synthesis and Reactivity in Inorganic, Metal-Organic, and Nano-Metal Chemistry, Vol 36, 2, pp. 231–235(5), 2006.

[7] AZoNanotechnology, http://www.azonano.com/details.asp?ArticleID=1818 (Last accessed 11 Nov 2009).

[8] AZoNanotechnology, http://www.azonano.com/details.asp?ArticleID=520 (Last accessed 11 Nov 2009).

[9] S. O. Kasap, *Principles of Electronic Materials and Devices 3rd Edition*, McGraw Hill, Chapter 2, pp. 154,.2006,.

[10] S. O. Kasap, *Principles of Electronic Materials and Devices 3rd Edition*, McGraw Hill, Chapter 2, pp. 155, 2006,.

[11] K.K. Ng, *Complete Guide to Semiconductors Devices*, McGraw Hill, 1995.

[12] S.M. Sze, *Modern Semiconductor Device Physics*, Wiley-Interscience, 1998.

[13] S.M. Sze, *Physics of Semiconductor Devices 2nd Edition*, Wiley Interscience. 1981.

[14] K.O. Leedy, *A bibliography on electron beam induced current analysis of semiconductor devices*, Solid State Technology, pp. 45–48, February 1977.

[15] Dimitris E. Ioannou, Charalabos A. Dimitriadis, *A SEM-EBIC minority-carrier diffusion-length measurement technique*, IEEE Transactions on Electron Devices, Vol. Ed 29, No 3, March1982.

[16] B.G.Yacobi and D.B.Holt, *Cathodoluminescence Microscopy of Inorganic Solids*, Plenum Press. 1990. Chapter 4.2 p. 59.

[17] H.J. Leamy, *Charge collection scanning electron microscopy*, J.Appl. Phys, 53(6), June 1982.

[18] "Learn NSOM". Nanonics Imaging Ltd. <http://www.nanonics.co.il> (Last accessed on 14 Oct)

[19] L.M.Mansfield, K.A. Bertness, P.T. Blanchard, T.E.Harvey, A.W.Sanders and N.A.Sanford, *GaN Nanowire Carrier Concentration Calculated from Light and Dark Resistance Measurements*, Journal of Electronic Materials, Vol 38, No 4. 2009.

[20] Stephen D.Winchell, *Transport Imaging in the One Dimensional Limit*, Master's Thesis, NPS. June 2006.

[21] Goldstein, Joseph and others, *Scanning Electron Microscopy and X-Ray Microanalysis 3rd Ed*, Kleiner Academic — Plenum Publishers.

[22] Wikipedia, http://en.wikipedia.org/wiki/Vapor-Liquid-Solid_method (Last accessed on 26 Oct 2009).

[23] Ilke Arslan, A.Alec Talin and George T. Wang, *Three-Dimensional Visualisation of Surface Defects in Core-Shell Nanowires*, The Journal of Physical Chemistry Letters, Vol 112, 2008, 11093–11097.

[24] A.Alec Talin, George T. Wang, Elain Lai and Richard J. Anderson, *Correlation of Growth temperature, Photoluminescence, and Resistivity in GaN Nanowires*, Applied Physics Letters, 92, 093105, 2008.

[25] Geroge T. Wang, Qiming Li, A.Alec Talin, Andrew Armstrong, Yong Lin and Jianyu Huang, *GaN Nanowires: Growth, Charaterization and Applications*, ECS Transactions, 2009 Vol 1.

[26] ImageJ, http://rsbweb.nih.gov/ij/ (Last accessed on 26 Oct 2009).

[27] Qiming Li, J.Randall Creighton and George T. Wang, *The Role of Collisions in the Aligned Growth of Vertical Nanowires*, Journal of Crystal Growth 310, 3706–3709, 2008.

[28] George T. Wang, A Alec Talin and others, *Highly Aligned, Template-free growth and Characterization of Vertical GaN Nanowires on Sapphire by Metal-Organic Chemical Vapor Deposition*, Nanotechonology, Vol 17, 5773–5780, 2006.

[29] Qiming Li and Geroge T. Wang, *Improvement in Aligned GaN Nanowire Growth Using Submonolayer Ni Catalyst Films*, Applied Physics Letters, 93, 043119, 2008.

[30] A. Alec Talin, Francois Leonard, B.S.Swartzentruber, Xin Wang, Stephen D.Hersee, *Unusually strong space-charge-limited current in thin wires*, Physics Review Letters, Vol 10, Issue 7, Article 076802, Aug 2008.

[31] Lee Baird, "*Near Field Imaging of Gallium Nitride Nanowires for Characterization of Minority Charge Carrier Diffusion,*" Master's Thesis, Naval Postgraduate School, Dec 2009.

THIS PAGE INTENTIONALLY LEFT BLANK

INITIAL DISTRIBUTION LIST

1. Defense Technical Information Center
   Ft. Belvoir, Virginia

2. Dudley Knox Library
   Naval Postgraduate School
   Monterey, California

3. Professor Andres Larraza
   Department of Physics, Naval Postgraduate School
   Monterey, California

4. Professor Nancy M. Haegel
   Naval Postgraduate School
   Monterey, California

5. Professor Gamani Karunasiri
   Naval Postgraduate School
   Monterey, California

6. Professor Yeo Tat Soon, Director
   Temasek Defence Systems Institute, National University of Singapore
   Republic of Singapore

7. Ms. Tan Lai Poh Assistant Manager
   Temasek Defence Systems Institute, National University of Singapore
   Republic of Singapore